ENERGY
www.csiro.au

Water contamination risk assessment on hydraulic fracturing in unconventional gas extraction

Raman Pandurangan, Dane Kasperczyk, James Kear, Zuorong Chen
EP179212
August 2018

ISBN (print) 978-1-4863-1006-7
ISBN (online) 978-1-4863-1007-4

Citation

Pandurangan V., Kasperczyk D., Kear J. and Chen Z. (2018) Water contamination risk assessment on hydraulic fracturing in unconventional gas extraction. CSIRO, Australia.

Copyright

Important disclaimer

Contents

Figures

Tables

Acknowledgements

This report was supported by the Gas Industry Social and Environmental Research Alliance (GISERA). GISERA is a collaboration between CSIRO, Commonwealth and state governments and industry established to undertake publicly-reported independent research. The purpose of GISERA is to provide quality assured scientific research and information to communities living in gas development regions focusing on social and environmental topics including: groundwater and surface water, biodiversity, land management, the marine environment, and socio-economic impacts. The governance structure for GISERA is designed to provide for and protect research independence and transparency of research. Visit gisera.csiro.au for more information about GISERA's governance structure, projects and research findings.

Executive summary

Concern over environmental impacts to groundwater resources due to wellbore delamination and hydraulic fracturing continues to be a challenge for the industry to effectively address despite low historical barrier, low well failure rates and a high standard of operation by the industry in Australia.

The aim of this project was to assess worst-case water resource risks due to hydraulic fracturing activities for the Surat basin and wellbore delamination for both the Sydney Basin in NSW and the Surat basin in Queensland. The focus on worst-case scenarios here provides advice that can be used to review state government regulation to ensure risks are maintained low and ongoing high operational standards are achieved by industry. Mathematical models are used in this study to quantify the risk magnitude associated with hydraulic fracture growth and well integrity. The risk magnitude and the associated uncertainty can be used to formulate risk management plans that minimise residual risk and inform community discussions.

Probability bound analysis (PBA) has been used to model hydraulic fracturing and wellbore delamination risks under best case and worst case scenarios. The PBA approach can be applied to all unconventional operations; however, this project focuses on coal seam gas (CSG) data and activities.

The hydraulic fracturing study in the Surat basin indicated that there is an 83% likelihood for the hydraulic fracture length to always be less than 500m and 74% likelihood that the hydraulic fracture height will always be less than 100m. However, it is not valid to conclude from these results whether hydraulic fractures would or would not intersect overlying aquifers or a nearby wellbore. These results should not be taken as an exact measure of the maximum fracture length or the height under field conditions. Fracture growth during hydraulic fracture operations in the field are monitored and fracture growth is suspended or abandoned when conditions indicate pressures cannot be maintained in a well. However, this information can be used as a starting point to determine setback distances and best practice operations to guide operators.

The wellbore delamination model shows that the risk of contamination to overlying aquifers is low for the Sydney and Surat basins. Post-decommissioning micro-annuli were estimated to have an opening less than 50 microns and be filled with water with low likelihood of significant gas flux through the micro-annulus. The potential for gas leak from a micro-annulus, if it exists, is therefore considered negligible and that interface debonding will not result in any significant contamination due to the hydraulic fracturing process.

The likelihood and quantitative estimates presented in this report can be expanded upon to be used by regulators to critically assess current projects and understand potential impacts on ground water resources, and accordingly develop a mitigation plan to reduce risks to acceptable levels.

1 Introduction

Hydraulic fracturing is an established technology used in the production of oil and gas from unconventional reservoirs, however there are often concerns raised about its environmental implications. These concerns commonly include air pollution, contamination of water bodies by chemical additives, soil contamination due to spills and leaks, waste water disposal, induced seismic events, and aquifer interaction. A key concern is water pollution for agricultural communities who fear that local gas production could have the potential to negatively impact water quality in local aquifers relied on for irrigation and livestock farming (O'Kane 2014).

It is important for communities living in regions where there is the potential for gas development to be provided with information on the risk of surface and groundwater contamination through transport of geogenic or introduced chemicals from drilling and hydraulic fracturing activities. The inadvertent stimulation of conductive pathways between production depths and surface or groundwater assets is another key concern for community groups who rely on the water resources. Traditional risk assessment methods have relied on either analysis of historical data or the technical investigation of a specific case (either where high quality data exists from an international location or an artificial worst-case scenario). These methods traditionally rely on empirical models formulated based on existing data to generate the likelihood of potential contamination. Alternatively, the analysis of a specific case does not provide a range of potential outcomes at a local or field scale. Without the quantitative information of risk likelihoods, it is difficult to both investigate the differences in contamination risk for different regions and prioritise expenditure into the most effective risk mitigation efforts (so that the most effective mitigation options can be implemented).

This project provides quantitative information on the contamination risk profile at a basin scale and identify key parameters that increase or reduce the likelihood of inadvertent stimulation of key conductive pathways of geogenic and hydraulic fracturing fluids to aquifers. The project focuses on two key potential conductive pathways: wellbore delamination and hydraulic fracture stimulation.

This project was developed from a discussion in June 2016 with the Office of Water Science, Department of the Environment and Energy in Adelaide. The Office of Water Science is leading the Australian Government's efforts to improve understanding of the water-related impacts of coal seam gas and large coal mining developments. This project addresses the following concerns and recommendations from the NSW Chief Scientist Review (O'Kane 2014), and specifically addresses stakeholder concerns and recommendations 11, 12 and 13 centred on risk prediction and management in Australian onshore gas industries.

- Stakeholders Concerns - How CSG development and particularly processes such as hydraulic stimulation ('fracking') will negatively affect agriculture land by depleting aquifers and ground water resources.
- There are things we need to know more about: To understand the risk of pollution and potential short- or long-term environmental damage from CSG and related operations.

- Recommendation 11: centralised Risk Management and Prediction Tool for extractive industries in NSW. Improving prediction capability of risk likelihoods.
- Recommendation 12: Updating and refining the Risk Management and Prediction Tool. On whether or not other unconventional gas extraction (shale gas, tight gas) industries should be allowed to proceed in NSW and, if so, under what conditions
- Recommendation 13: Companies or organisations seeking to mine, extract CSG or irrigate as part of their initial and ongoing approvals processes should, in concert with the regulator, identify impacts to water resources, their pathways, their consequence and their likelihood, as well as the baseline conditions and their risk trigger thresholds before activities can start.

This project will introduce the engineering processes that exist as part of hydraulic fracturing. The aim of this project is to identify likelihoods so that the information can be used by industry and government to reduce risks and inform communities of the quantitative extent of hydraulic fracturing activities. In this project, hydraulic fracturing models, uncertainty quantification techniques and historical data have been used to generate a likelihood of potential contamination scenarios.

1.1 Hydraulic fracturing

Hydraulic fracturing is a technique that has been used to improve oil and gas reservoirs production since the late 1940s (Montgomery and Smith 2010). Hydraulic fracturing involves the injection of a fracturing fluid into a target formation in order to increase the permeability of the formation and allow extraction of hydrocarbons. The hydraulic fracturing fluids used are predominantly a mixture of water, proppant (usually sand), and small percentage of chemical additives (typically less than 1%). The zone to be fractured is often known as the pay zone, and the wellbore casing this zone is perforated and then isolated using mechanical plugs or other devices, before the hydraulic fracturing fluid is injected into the isolated wellbore zone. Hydraulic fracturing fluid is pumped into the isolated wellbore zone until pressure exceeds a threshold known as the breakdown pressure. Once the hydraulic fracture fluid pressure exceeds the breakdown pressure it fractures the rock resulting in *hydraulic* fractures or reopens existing fractures.

The direction the fracture grows depends on the orientation of the stress in the reservoir, with growth mainly occurring in a direction perpendicular to the minimal principal stress. The size or volume of the fractures is determined by how much hydraulic fracturing fluid stays in the fracture. As the volume of hydraulic fractures grow some of the injected fluid can be absorbed by the formation via a process known as leak-off. The fluid injection rate is calculated to propagate hydraulic fractures to the desired size given the expected fluid leak-off into the formation. The goal of hydraulic fracture design is to optimize the treatment so as to arrive at a fracture length and pathway that maximizes productivity but minimizes treatment costs. Further information about the hydraulic fracturing process and the use or proppants, can be found at https://gisera.csiro.au/more-information/frequently-asked-questions/how-is-onshore-gas-extracted/.

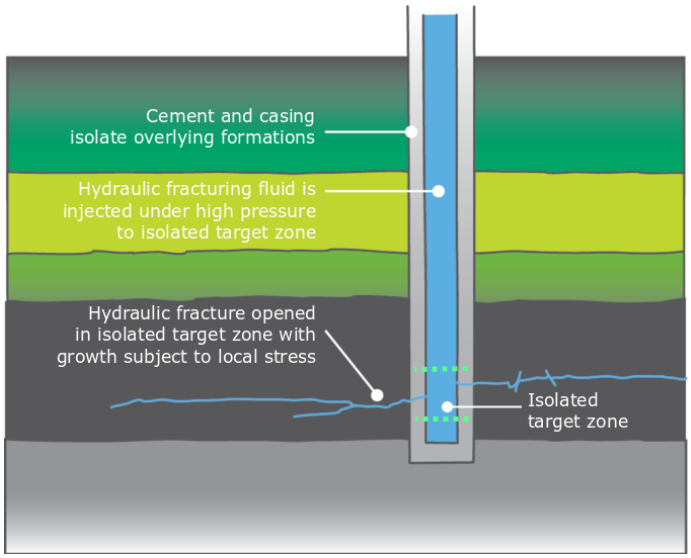

Figure 1 - Diagram of hydraulic fracturing process in a targeted zone such as a coal seam

Source: Adapted from GISERA, 2018

1.2 Wellbore integrity

Wellbores are deep vertical holes drilled into the earth to extract oil and gas and are designed to prevent unintended fluid migration between different geological formations (known as well integrity). Well integrity is an important aspect of well operations that is critical for maintaining the safe operation of the well and to protect the environment.

Once a well is drilled, a steel casing string is run into the wellhole and cemented into the ground (Figure 2). The cement barrier fills and seals the space (annulus) between the steel casing string and the surrounding rock or between one casing string and another. The cement barrier is crucial for maintaining the wellbore integrity (Huddlestone-Holmes et, al. 2017) and has three basic functions:

1. Firstly, it prevents fluid movement up and down along the outside of the wellbore between different geological formations (zonal isolation).
2. Secondly, the cement protects the steel casing from corrosion from formation fluids, and
3. Finally it provides mechanical support for both the casing and the formation (Taoutaou 2010).

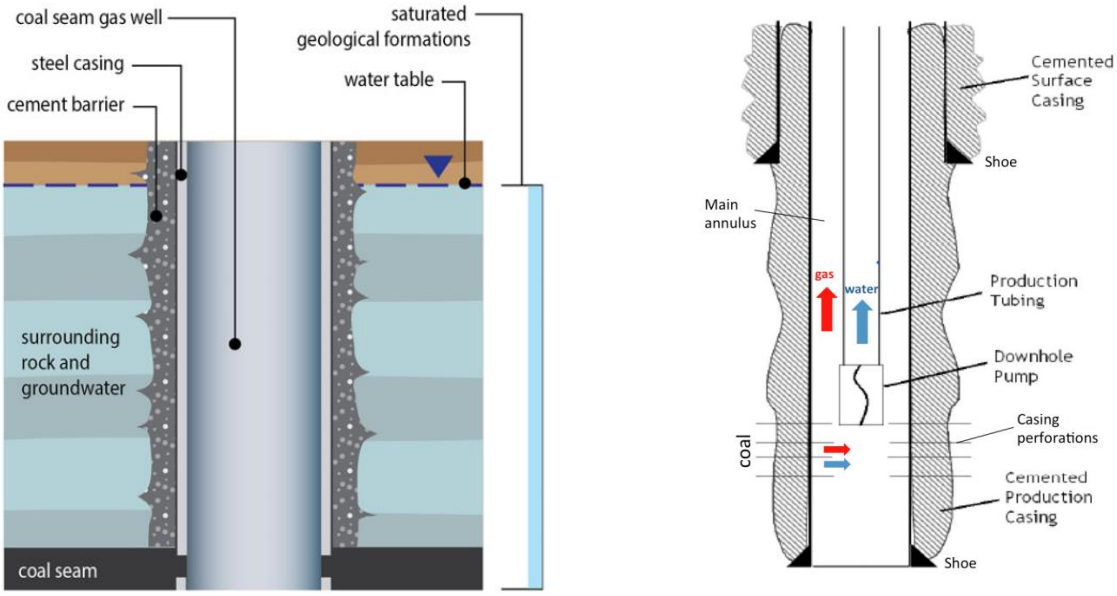

Figure 2 - (Left) Schematic of a CSG well adapted from NSW Office of Water (2013) 'How Coal Seam Gas is Extracted in NSW', Factsheet 2, and Department of Primary Industries. (Right) CSG well design (Gasfields Commission 2014)

The ISO standard petroleum and natural gas industries - Well integrity - Part 1: Life cycle governance (**ISO 16530:1 2017**) defines well integrity as "*maintaining full control of fluids within a well at all times by employing and maintaining one or more well barriers to prevent unintended fluid movement between formations with different pressure regimes or loss of containment to the environment*."

Well barriers consist of elements that contain fluids within a well and prevent uncontrolled flow within or out of the well. Well barriers can include physical or hardware barriers, operational barriers, human barriers and administrative barriers. For example, physical barrier may include

impermeable formations, drilling fluids, casing cement, casing strings, packers, wellheads and valves, and blowout preventers.

Well integrity can be compromised by poor cementing, leaking through casing connections, cement sheath degradation and casing corrosion which may allow oil, gas, or water to migrate along the wellbore annulus. In such a situation, the wellbore in itself can act as a potential pathway through which fluids and hydrocarbons from the reservoir could leak into a low pressure zone such as an overlying aquifer or to the atmosphere.

1.3 Unconventional Gas Sector in Australia

Oil and gas account for 68% of Australia's primary energy consumption with natural gas alone accounting for 24% of that total (Office of the Chief Economist 2016). Unconventional gas development in Australia includes coal seam gas, tight gas and shale gas. Further information on unconventional gas definitions can be found at https://gisera.csiro.au/more-information/frequently-asked-questions/what-is-coal-seam-gas/. In the 2015/16 financial year 986 PJ of gas was produced from coal seam gas (CSG) with more than 95% of this in Queensland (DNRME 2017a) and little to no production in shale or tight gas.

Table 1 - Proven and produced unconventional gas resources in Australia
Source: Geoscience Australia 2016

Resource	Reserves (PJ)	Identified resources (PJ)	Production 2015-16 (PJ / year)
Coal Seam Gas	45,949	79,583	986
Tight Gas	39	1,748	0
Shale Gas	0	12,252	0

Many Australian sedimentary basins are prospective for unconventional gas with around 46,000 PJ of unconventional gas reserves in CSG, tight gas and shale gas (Geoscience Australia 2016). Table 1 shows the current proven and produced gas resources in Australian basins. Potential CSG basins and major CSG exploration include areas such as the Galilee basin, Gunnedah basin and Sydney basin (Figure 3).

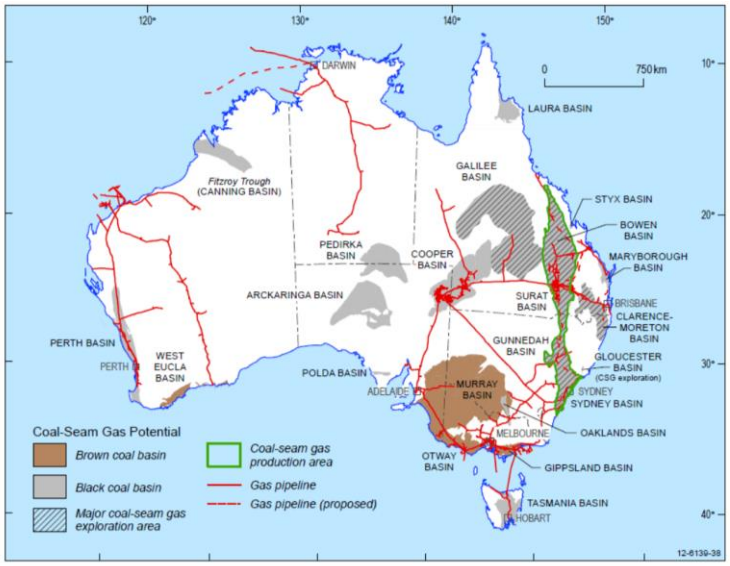

Figure 3 - Potential and current producing Coal Seam Gas basins in Australia

Source: Geoscience Australia and BREE 2012 © Commonwealth of Australia (Geoscience Australia).

Australia has significant unconventional resources, however, due to geological challenges, cost of development, social and environmental objections production has not grown as quickly as expected (Cook et al. 2013). Investment and expansion particularly slowed due to changes to legislation, responses to community/regional concerns and changes in in market conditions (Cook et al. 2013; Maloney 2015; Department of Natural Resources and Mines 2016). State and territory governments are responsible for regulating unconventional gas activities with some states legislating temporary bans on the development of onshore gas and/or the use of hydraulic fracturing for gas extraction. Though some of these state wide bans have been lifted, states such as Victoria have an imposed ban on hydraulic fracturing and a moratorium on onshore gas development until 30 June 2020 (Parliament of Victoria 2017). The Australian Independent Expert Scientific Committee on Coal Seam Gas and Large Coal Mining Development (IESC) was established in 2012 assist the industry growth and to provide advice on all CSG projects.

CSG development began in Queensland with the first gas production from the Bowen Basin in 1997. A rapid expansion in CSG production occurred after three major projects were brought into production; Australia Pacific LNG (APLNG), Gladstone LNG and Queensland Curtis LNG (Sander et al. 2014). Associated to these projects Queensland CSG production increased from 280 PJ in 2013-14 to 979 PJ in 2015-16.

2 Potential hazards associated with CSG extraction

A hazard analysis conducted for the Clarence-Moreton bioregion as part of the Bioregional assessment programme identified 226 CSG-related activities during stages of CSG project development, from exploration to decommissioning, that could potentially negatively impact the quality and/or quantity of surface and ground water resources (Raiber et al. 2016). Among the hazardous activities identified were: compromised integrity of well cement, hydraulic fracture direct contamination of non-target aquifers, hydraulic fracture dilation of flow pathways to overlying aquifers and hydraulic fracture dilation of wellbore conductivity causing leakage to the surface. Sections 2.1 and 2.2 provide an overview of hydraulic fracturing and well integrity and how they relate to water resources.

2.1 Hydraulic fracturing for gas extraction

Access to unconventional gas resources typically require technologies such as hydraulic fracturing to extract them from complex formations with low permeability, however in areas of high permeability no hydraulically fracturing is required. Across all wells in Queensland, the only state with a large sample size, hydraulic fracturing is used in about 10% of wells (DNRME 2018).

Detailed inquiries have been conducted by almost every Austrian state and territory to identify the impacts of onshore unconventional gas development on the economy, environment and the society (O'Kane 2014; Office of the Chief Economist 2015; Tas. Department of Primary Industries, Parks, Water and Environment 2015; Vic. Environment and Planning Committee 2015; WA Standing Committee on Environment and Public Affairs 2015; SA Parliament, Natural Resources Committee 2016; NT Parliament 2017). The potential threats which have been identified in these inquiries include, contamination of surface and ground water sources, decrease in air quality, issues related to land usage, greenhouse gas emissions, induced seismicity, impact on human health, disruptions to Aboriginal culture, and degradation of terrestrial and aquatic ecosystems.

Recent studies have also looked into the possibility of shallow groundwater contamination due to hydraulic fracturing fluid migration along conductive faults in shale. (Birdsell et al. 2015) provide a review on the recent literature on this topic and use transport simulations to quantify the amount of fracturing fluid that reaches an overlying aquifer. Based on their study, they conclude that the likelihood of hydraulic fracturing reaching water resources is low when the vertical separation between the hydraulic fracturing zone and the water body is large and other natural pathways such faults or leaky wells are absent. Their results show upward migration in the order of 100m through relatively low-permeability overburden, even in the absence of permeable pathway. They also highlight reported instances of fluid migration that have occurred in the past and the need for detailed modelling approaches that can explain these happenings. The finding of this study has also been cited by the recent US EPA report (U.S. EPA 2016). In the case of deep shale formations the vertical separation distance is the order of thousands of meters, and it is unlikely for hydraulic fractures to grow through thousands of maters of rock into underground drinking water resources. However, risk quantifying becomes important when groundwater and gas resources are co-located

such as in CSG where CSG resources and groundwater resources have relatively small separation distances. Most risk assessment studies completed on hydraulic fracturing focus on risk identification and risk legislation with little research found on risk quantification. Therefore, the objective of this study is to arrive at quantitative estimates on the contamination risk profile at a basin scale, and inform sections in the risk assessment exercise which currently lack quantification.

2.2 Well integrity

There are many mechanisms that may result in well integrity failure, which can have a range of environmental impacts such as contamination of aquifers or fugitive gas emissions. Well integrity failures can take one of the following forms

- Well breach (including failure of cement sheaths/plugs/bonds, casing, and downhole and surface sealing components);
- Hydrological breach (fluid movement between geological formations – including formations not targeted for exploitation); and
- Environmental breach (contamination of or water balance impact to water resources – fluid leaks at surface and causes contamination of water sources).

Maintaining the integrity of oil and gas wells is important as leakage of gas or hydrocarbons can have significant health, safety, environmental and financial implications (Miyazaki 2009). Recent studies in United States have looked into the methane gas leaks into the atmosphere and/or into underground sources of drinking water due to loss of well integrity, which often raises serious environmental concerns (Moore et al. 2012; Jackson et al. 2013; Ingraffea et al. 2014).

The integrity of the cement is therefore of utmost importance to ensure that overall wellbore integrity is maintained and contamination risks are minimized. Cement failure has been identified during the life of wells generating leakage pathways between the casing and the formation (Fourmaintraux et al. 2005). The impact if such a failure occurred depends on the extent of the local geological conditions. For example, a study in the Gulf of Mexico found that there was no breach in isolation between formations with pressure differentials as high as 97 MPa, as long as 15m of high quality cement seal was present between the formations (Bonett and Pafitis 1996).

2.2.1 Wellbore integrity failure mechanisms

Debonding of the cement/casing or cement/rock interfaces is known as micro-annulus growth. The two potential drivers of this micro-annulus growth considered in this report are: high cyclic pressures exerted on the well during hydraulic fracturing operations and long term pore-pressures after decommissioning.

2.2.1.1 Wellbore integrity failure – High cyclic pressures exerted on the well during hydraulic fracturing operations

Wellbores must be designed and constructed to withstand the high cyclic pressures exerted during hydraulic fracturing operations otherwise these pressures would potentially damage the cement seal or the steel casing leading a to breach of the inter-aquifer seal (US EPA 2015). According to Behrmann and Nolte (1998), a micro-annulus is usually present after hydraulic fracturing treatments

in sections of the wellbore which are exposed to casing perforation operations and hydraulic fracturing fluid pressure. As with other modes of cement barrier integrity failure, if this hydraulic fracturing induced micro-annulus has grown sufficiently large so as to intersect other geological layers, it may act as a conduit for fluids, particularly gas (like methane or CO_2 with low densities) to migrate (Dusseault et al. 2000). It must be noted however that although gas migration along a micro-annulus appears to be the most likely cement barrier integrity issue, the leakage rate is likely to be very low because of the limited aperture of this micro-annulus pathway and limited driving mechanism. The expected length and aperture of this hydraulic fracturing induced micro-annulus in the Surat basin has been modelled in Section 6.2.1.

2.2.1.2 Wellbore integrity failure – Decommissioned wells

If a decommissioned oil and gas well loses wellbore integrity a leak may develop over time. This loss of wellbore integrity may be accelerated if the wellbore intersects geological layers with high residual pressures such as formations used for underground gas storage or formations where ground movement from repeated cycles of injection and extraction of gas serve to weaken the cement barrier (Miyazaki 2009). Well leakage/integrity failure in decommissioned wells has also been attributed to poorly cemented casing, casing failure and cement plug failure.

In decommissioned wells with compromised wellbore integrity, the interfaces between the cement barrier and the formation rock and/or the steel casing could act as preferential pathways for fluid migration to the surface. In addition, failure of the outer cement barrier could also act as a pathway for fluid migration into natural fractures, faults and overlying formations (Zhang and Bachu 2011). The expected aperture of the pore pressure induced micro-annulus has been modelled in Section 6.2.2.

2.2.1.3 Other wellbore integrity failure mechanisms – Drilling induced failure

Drilling induced failure of the wellbore can be caused if the pressure of the drilling fluid (known as drilling mud) is not in balance with the formation pore fluid pressure in the surrounding rock. If the drilling mud pressure is significantly lower than the formation pore fluid pressure (low mud weight), the formation fluid will flow into the well and can force the drilling mud back to the surface (known as a well blowout). Low mud weight can also result in an enlarged wellbore that may result in poor displacement of mud during cementing and poor quality cement sheath behind the steel casing leading to a potential loss of well integrity. If the drilling mud pressure is greater than the formation fluid pressure it can lead to the loss of drilling mud into the surrounding formations or reservoirs and in severe cases, unintended fracturing of the formation. Drilling induced wellbore failure mechanisms have not been investigated in this report.

2.2.1.4 Other wellbore integrity failure mechanisms – Cement completions

Cement barriers and cement decommissioning plugs for critical components of wellbore integrity. Typically the cement barrier has a low permeability and hydraulic conductivity, and bonds well to the steel casing and rock surfaces preventing the migration of fluids (Parcevaux et al. 1990). However, defects in or failure of these cement components can occur due to poor cement placement, low cement quality or improper well completion.

Defects or failures within the cement barrier or at the interfaces can create a preferential pathway for fluid migration in any of the following forms: a mud channel caused by improper cement placement, cracks which develop in the cement during the curing process, or micro-annuli debonding between cement/casing or cement/rock interfaces (Watson and Bachu 2009; Loizzo et al. 2011).

Cement shrinks as it cures and if the design and placement of the wellbore cement components is not fit for purpose, this cement shrinkage can result in a micro-annulus debonding along the interface between cement barrier and steel casing and/or between the cement barrier and the surrounding rock. Changes to downhole pressure and temperature during the life cycle of the well can induce radial deformation of the steel casing and failure in the cement barrier, resulting in micro-annuli debonding on the interfaces between cement sheath and casing/formation, creating radial fractures and migration pathways (Goodwin and Crook 1992; Watson et al. 2002). Cement completions induced wellbore failure mechanisms have not been investigated in this report.

2.2.2 International well integrity data

If a well integrity failure is observed or suspected to have developed, technologies, tools and mitigation measures are available to confirm the failure mechanisms, identify their extent, and conduct mitigation operations at an optimal time. The NSW chief scientist report notes that the risk of long-term leakage from the CSG wells from both the casing and cement can be considered to be minimal, although there is scope for additional research to specifically assess the impact of abandoned CSG wells over an extended timeframe (O'Kane 2014).

Davies et al. (2014) provide a detailed summary of well barrier and well integrity failures based on publicly available data, and have reported a well barrier and integrity failure rate ranging from 1.9% to 75%. However, the results have been criticised as it does not differentiate cases of barrier failure (where fluids would still be contained by other the well barriers) from cases of well integrity failure that lead to an environment contamination (Thorogood and Younger 2015). Ingraffea et al. (2014) conducted a risk assessment for casing and cement impairments which can lead to methane migration into the atmosphere and/or into underground sources of drinking water, based on data collected from conventional and unconventional oil and gas wells drilled in Pennsylvania, USA between 2000 and 2012, and have reported a well failure rate between 0.73% to 9.84%. However, it was pointed out that not all the wells issued with a notice of violation will result in groundwater contamination.

2.2.3 Australian well integrity data

In the Australian context, there have been few estimates made for failure rates for CSG wells. The report from the (GasFields Commission 2014), provides key statistics based well integrity compliance auditing corresponding to 6,734 CSG wells drilled between 2010 to March 2015. The auditing involved both subsurface gas well compliance and surface well head compliance testing. For the subsurface equipment, no leaks were reported while there have been 21 statutory notifications (a rate of 0.3%) concerning suspect downhole cement quality during construction. After remediation, the cement failure rate was determined to be zero. For subsurface equipment, the risk of a subsurface breach of well integrity is assessed to be very low to near zero. In regards to

the surface well head leaks, 199 leaks of surface equipment have been reported and have been subsequently fixed. (Patel et al. 2015) reported a study on well integrity issues for all onshore oil and gas wells drilled in Western Australia and found that 122 wells out of 1035 (12%) non-decommissioned wells have compromised barrier integrity, but none of them had leakage. Tubing failure accounted for a majority of these barrier failures (8.3%) and production casing failure accounted for a small percentage of the total (2%). Tubing leaks can occur through holes corroded by production and injected fluid inside the tubing or from twisting of the tubing, while casing failure occurs predominantly in production casing due to corrosion, pressure differential and thermal effects.

3 Overview of case study regions

This report focuses on two regions for assessment; the Surat Basin in Queensland (QLD) and the Sydney Basin in New South Wales (NSW). Section 3.1 and 3.2 provide an introduction of each basins, current and potential CSG production, and a brief overview of the typical stratigraphy found across the basins. Input data collected from each of these case study regions can be found in section 5.

3.1 Surat Basin, Queensland

The Surat Basin is located in central southern QLD stretching into northern central NSW (Figure 4). This project explores the QLD section of the Surat basin which encompasses around 180,000 square kilometres.

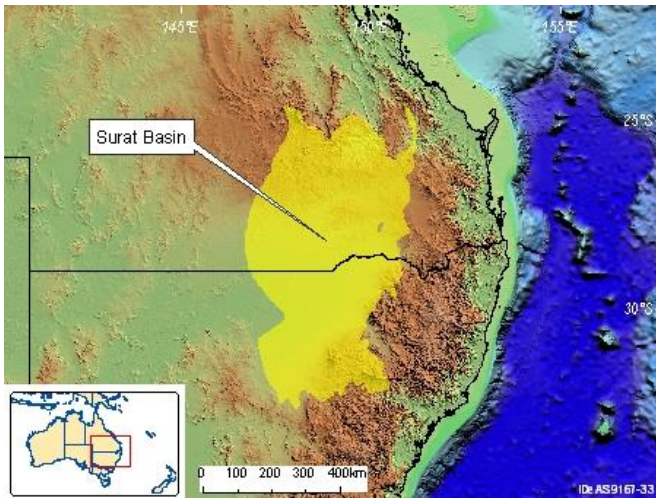

Figure 4 - Surat Basin map overview
Source: Geoscience Australia 2017 © Commonwealth of Australia (Geoscience Australia) 2017.

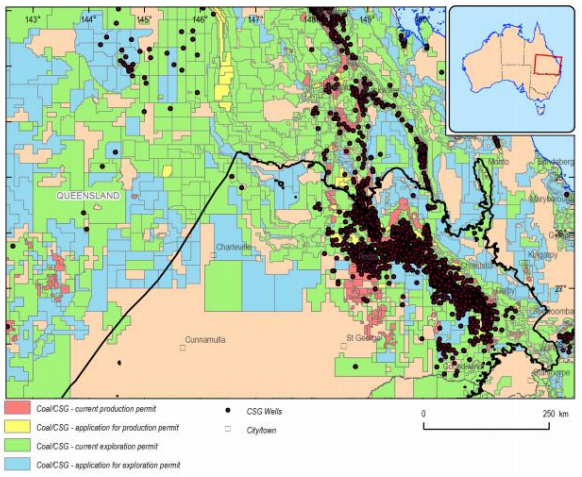

Figure 5 - Distribution of CSG wells in QLD Surat Basin and surrounds
Adapted from Ransley et al. (2015)

The coal formations in the Surat Basin are not as deep as nearby basins and the shallower depths have been a target for CSG development (Queensland Competition Authority 2014). Figure 5 shows the distribution of the CSG well in the Surat basin along concentrated on the east side of the basin. The total gas produced from region increase 613 PJ between 2013/14 and 2015/16 (Figure 6).

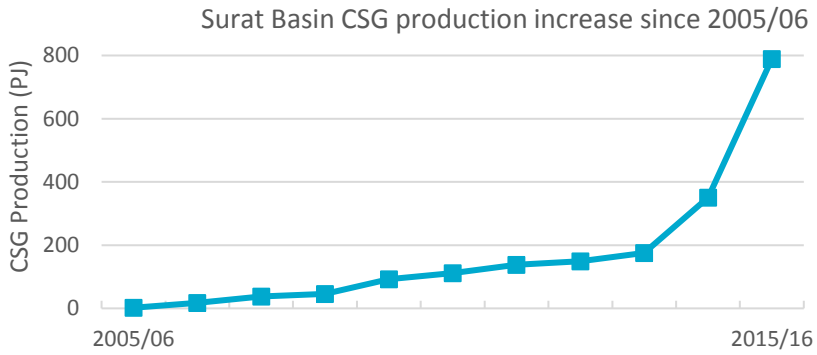

Figure 6 - CSG Production in Surat Basin per financial year
Source: Department of Natural Resources, Mines and Energy (2017a)

There is a potential for drilling over 20,000 CSG wells in the Surat basin and around 8,000 CSG wells have been drilled to May 2018 in the Surat and southern Bowen basin. (GasFields Commission 2018). Table 2 shows a list of the major projects that have been constructed or approved in the Surat basin. The list is not absolute, some of these projects have been indefinitely postponed and not all the wells would be stimulated by hydraulic fracturing. It is expected that across all projects between 5-20% of wellbores will need to be stimulated with hydraulic fracturing. Due to the nature of the target formation, some projects such as the Surat Gas Project would have no hydraulically fractured wells, while projects such as Dalwogan require 100% stimulation to be productive.

Table 2 - List of CSG projects and proposed number of wells
Source: QGC Limited (2009); Department of Environment and Energy (2013); Department of Environment (2014); Australia Pacific LNG Pty Limited. (2014); Department of Environment and Heritage Protection (2014). # includes current wells and any future approved wells.

Project	Status	Operator	Planned total number of wells#	Number expected to use hydraulic fracturing
Surat Gas Project	Approved	Arrow Energy	6500	0
Tipton	Expansion	Arrow Energy	270	No data
Western Surat Gas Project	Approved	Senex	425	0
Talinga / Orana	Production	APLNG	753	0
Condabri	Production	APLNG	726	0
Combabula, Ramyard	Production, Expansion	APLNG	2972	>380
Dalwogan	Expansion	APLNG	400	400
Gilbert Gully	Expansion	APLNG	925	>400
Woleebee	Construction	APLNG	285	285
Kainama	Construction	APLNG	284	>140
Spring Gully	Production	APLNG	465	No data
Peat	Production	APLNG	39	No data
Pine Hills	Production	APLNG	814	No data
QCLNG	Approved	QGC	6000	No data
Roma Field	Production	Santos	300	>100
Charlie	Approved	QGC	400	No data
Ironbark	Postponed	Origin	600	No data

The north-eastern boundary of the basin finds the outcrops of the Walloon coal subgroup which has seen the most intense CSG development. Figure 7 overlays the location of the majority of the CSG wells drilled within the bounds of the Surat basin as well as the upper depth of the Walloon subgroup. Majority of the wells are located in areas with a top Walloon subgroup between 0m-500m deep.

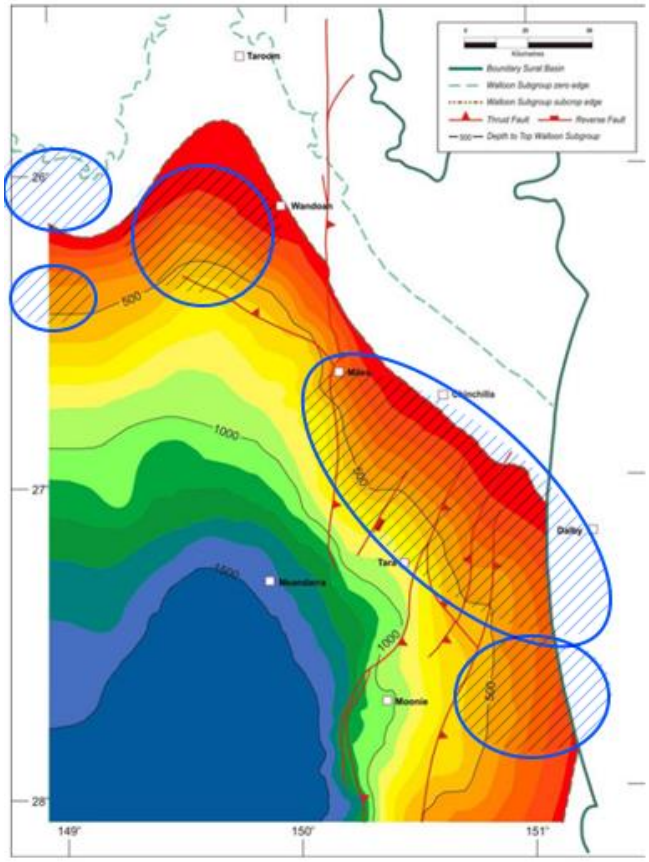

Figure 7 - Depth to top of Walloon subgroup from surface (Scott et al. 2007) overlayed with location of ~90%+ of coal seam gas appraisal and production wells (blue outline) based on data from Department of Natural Resources and Mines (2017b).

The complete stratigraphy of the Surat basin is shown in Figure 8. The main target for CSG production is the Last Jurassic Walloon Coal Measures. The Walloon Coal Measures, Springbok Sandstone, Hutton Sandstone and Precipice Sandstone have all been identified as gas prone formations in certain regions of the Surat Basin (Department of Natural Resources and Mines 2014). Significant groundwater volumes can be produced from the Springbok Sandstones (Arrow Energy 2012), and water quality is better in the shallower eastern Surat regions. The Condamine alluvium which is primarily used as a groundwater source lies above the tertiary sediments (Figure 9).

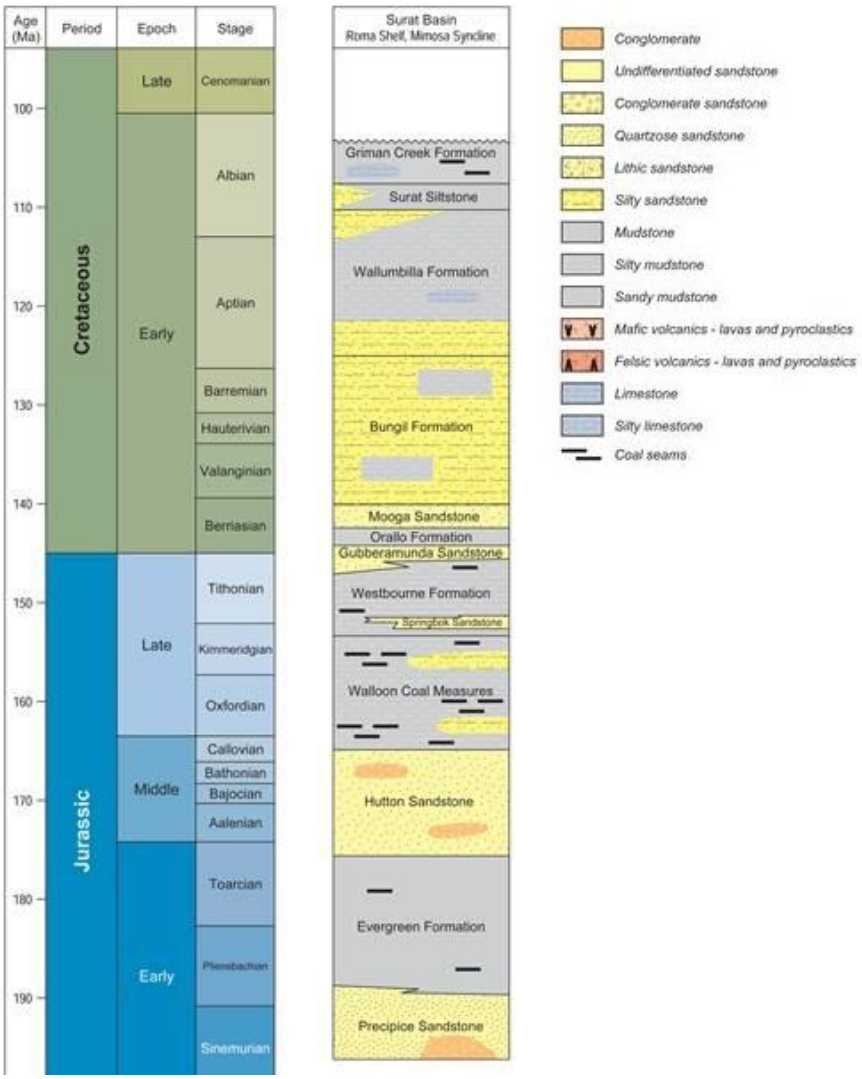

Figure 8 - Surat Basin stratigraphy (Welsh et al. 2014)

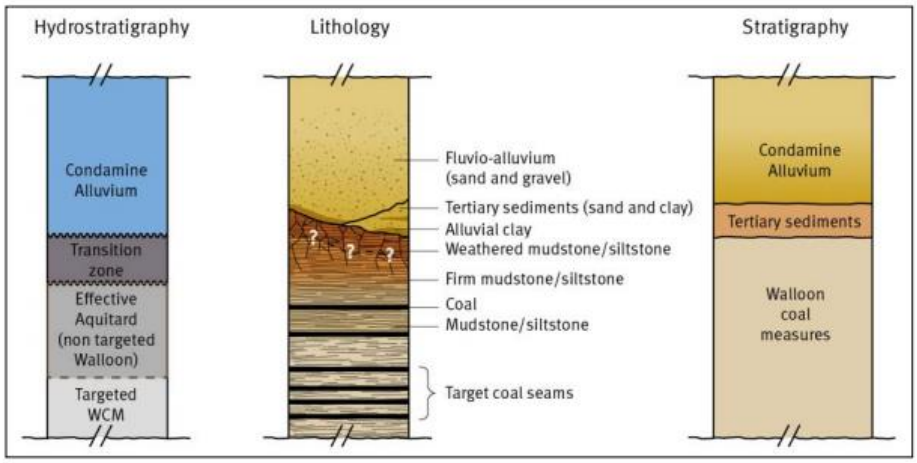

Figure 9 - Schematic showing the Condamine Alluvium above the Tertiary sediments (Office of Groundwater Impact Assessment 2016)

3.2 Sydney Basin, New South Wales

The Sydney basin is located in central eastern NSW and covers around 30,000 square kilometres onshore and 28,000 square kilometres offshore. The cities of Sydney, Newcastle and Wollongong along with other regional centres lie within the Sydney basin with a total residential population of over 5 million.

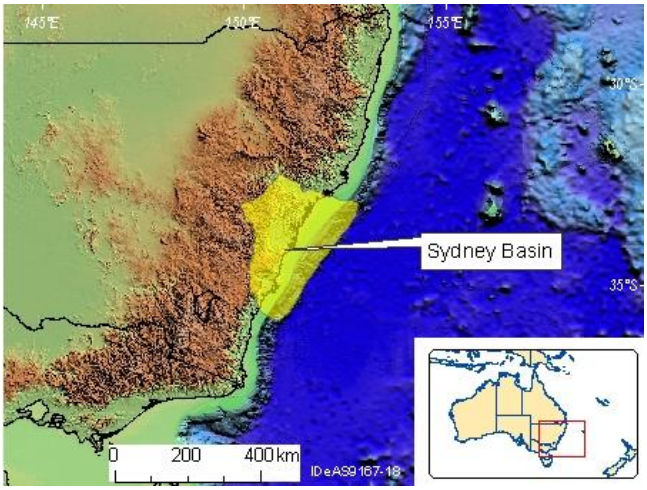

Figure 10 - Sydney Basin map overview
Source: Geoscience Australia (2017) © Commonwealth of Australia (Geoscience Australia) 2017.

Exploration wells have been drilled across the Sydney basin by operators such as AGL, Amoco Australia, Sydney Gas (Acquired by AGL in 2009) and Pacific Power since the early 1990s (Department of Industry NSW 2016). The Camden Gas Project is the only significant CSG project operating in the Sydney Basin which began production in 2001 and due to cease production in 2023 (Table 3). The project has a total of 153 wells of which around 75% are hydraulically fractured. Gas production from the Sydney basin provides ~6PJ a year, around 5% of NSW gas consumption (NSW Parliamentary Research Service 2013).

Table 3 - Sydney basin coal seam gas projects

Project	Status	Operator	Planned total number of wells	Percentage hydraulically fractured	Source
Camden Gas Project	Production	AGL	153	75%	(NSW Parliament 2011)

This project focuses on the Camden region within the Sydney basin, a region that has produced gas through hydraulic fracturing wells. The stratigraphy of the onshore Camden Gas project area is shown in Figure 11. The Illawarra Coal measures are the typical target formation for CSG development situated at an average depth of 670m. The major aquifers include the quaternary and tertiary alluvium deposits as well as the Hawksbury sandstone formation (AGL 2013).

Age	Unit			Lithology*	Average Thickness # (m)	Average depth to top# (m bgl)
Quaternary	Alluvium			Quartz and lithic "fluvial" sand, silt and clay	<20	0
Tertiary	Alluvium			High- level alluvium		
Triassic	Wianamatta Group		Bringelly Shale	Shale, carbonaceous claystone, laminite, lithic sandstone, rare coal	80 (top eroded)	0 -20
			Michinbury Sandstone	Sandy barrier island complex. Fine to medium-grained lithic sandstone.		
			Ashfield Shale	Black to light grey shale and laminite.		
	Mittagong Formation			Interbedded shale, laminite and medium-grained quartz sandstone.	11	113
	Hawkesbury Sandstone			Medium to coarse-grained quartz sandstone with minor shale and laminite lenses.	173	114
	Narrabeen Group	Gosford Subgroup	Newport Formation	Lower part contains quartzose sandstones which are top-sealed by the shaly laminite at the top of the unit.	35	274
			Garie Formation	Clay pellet sandstone.	8	308
		Clifton Subgroup	Bald Hill Claystone	Dominantly red shale and fine to medium-grained sandstone.	34	292
			Bulgo Sandstone	Fine to medium-grained quartz-lithic sandstone with lenticular shale interbeds.	251	331
			Stanwell Park Claystone	Red, green and grey shale and quartz-lithic sandstone.	36	574
			Scarborough Sandstone	Quartz-lithic sandstone, pebbly in parts.	20	621
			Wombarra Claystone	Grey shale, minor quartz-lithic sandstone.	32	636
Permian	Illawarra Coal Measures	Sydney Sub-group	Bulli Coal	Shale, quartz-lithic sandstone, conglomerate, chert, sporadically carbonaceous mudstone, coal and torbanite seams.	4	667
			Loddon Sandstone		12	684
			Balmain Coal Member		24	737
			Balgownie Coal		2	684
			(Remaining Sydney Sub-group)		?	699
		Cumberland Sub-group			-	-
	Shoalhaven Group			Sandstone, siltstone, shale, polymictic conglomerate, claystone; rare tuff, carbonate, evaporite.	-	-
Paleozoic	Lachlan Fold Belt			Intensely folded and faulted slates, phyllites, quartzite sandstones and minor limestones of Ordovician to Silurian age (PB, 2011a)	-	-

Key: * From Geoscience Australia's Stratigraphic Units Database (http://dbforms.ga.gov.au/www/geodx.strat_units.int); #average thickness and depth to top taken from available information on all wells within CGP

Figure 11 - Camden area stratigraphic table (AGL 2013)

4 Method

Risk is defined as the combination of possible consequences and associated uncertainty (Aven et al. 2007). An engineering approach to risk assessment combines:

1. risk identification to recognize threats,
2. risk analysis to understand the cause and nature of risk and arrive at quantitative estimates of the risk magnitude, and
3. risk evaluation to compare risk levels against set standards (ISO 31000:2009 2009).

This project will use risk assessment to arrive at quantitative estimates of risk at a basin scale, for two specific contamination pathways: hydraulic fracturing and wellbore delamination.

Probability bound analysis has been used to compute the bounds of contamination under the best case and worst case scenarios. This information can be used by regulators to assess ongoing or future projects, by organisations for risk assessment, and by communities to better understand the impact to water resources due to onshore gas development.

4.1 Probability bounds analysis

Risk analysis depend on parameters and inputs that have associated uncertainty. The uncertainties can be an aleatory, which is due to variability (known unknowns), or epistemic which refers to lack of information (known unknowns). Epistemic uncertainties can be reduced by further study, while aleatoric uncertainty is naturally present and often irreducible. Probability bound analysis (PBA) is a method used in risk analysis, that combines probability theory and interval arithmetic to propagate both aleatoric and epistemic uncertainty (Yager 1986; Frank et al. 1987; Williamson and Downs 1990; Ferson and Ginzburg 1996). This approach has been widely in solving environmental risk assessment problems (Sander et al. 2006; Rozell and Reaven 2012; Augustsson and Berger 2014; Betrie et al. 2015).

In this work probability bound analysis was carried out using *Risk Calc 4.0* software (Ferson 2000) that supports many named distributions and non-parametric models. While Monte Carlo methods approximate the probability distribution, the PBA approach bounds the true probability distribution of the uncertain parameter and does it at a fraction of the computational effort (Karanki et al. 2009). This method is particularly useful in situations where limited information is available about the parameters and shape of the distribution, or not much is known about their dependencies. For a detailed review of PBA, the readers are directed to the review paper by (Karanki et al. 2009).

A probability box (or p-box) is one way of representing uncertainty when both aleatoric and epistemic uncertainties are present (Ferson and Hajagos 2004). Appendix C: Probability box contains an example of creating a p-box with aleatoric and epistemic variables. The main advantage of using the *p-box* approach with a simple hydraulic fracture model is to provide first-hand estimates of the risk magnitude at a basin scale.

4.2 Hydraulic fracture model

For this study two hydraulic fracturing models were used to simulate different contamination pathway scenarios. The two scenarios investigated were a) intersecting a water bore and b) vertical fracture propagation. For the water bore scenario we use the PKN model as it predicts the maximum fracture length. The penny shaped model is used to predict vertical fracture propagation as it is not constrained vertically and predicts the maximum vertical propagation distance.

The PKN (Perkins– Kern–Nordgren) model (Perkins and Kern 1961; Nordgren 1972) is an analytical model for simulating the growth of a planar hydraulic fracture propagating in a direction perpendicular to the minimum in-situ stress at a fixed height (Figure 12). The PKN model was chosen to simulate a scenario where the fracture growth occurs within the coal seam and the fracture intersects a water bore at the same depth. In this case the fracture height can be assumed to be the same as pay-zone height. A detailed explanation of PKN is provided in Appendix A.

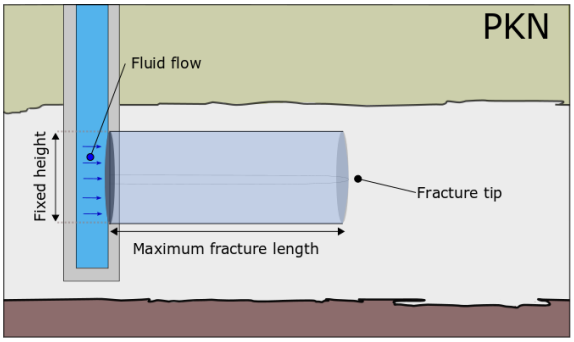

Figure 12 - Schematic of a PKN fracture

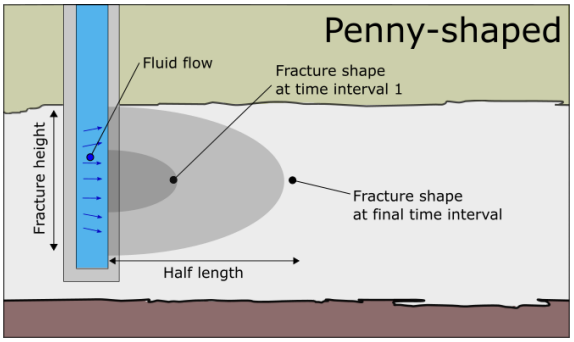

Figure 13 - Schematic of a Penny-shaped fracture

This study investigates the parameters that create maximum fracture height growth conditions. For a given fracture volume a shorter fracture length results in a larger fracture height. The penny shaped model is used for the vertical fracture propagation and is appropriate when the height growth is not constrained or when the fractures are horizontal. In the penny-shaped model the hydraulic fracture is not artificially constrained within the coal layer and is allowed to grow in a circular shape (Figure 13). Fracture height growth under actual field conditions can be influenced by several factors such as the local geology, the presence of natural fractures or faults, local variation in *the in-situ* stresses, material heterogeneity, and it is difficult to capture all these factors using a numerical model. Therefore, the penny shaped model gives a conservative estimate for the fracture height that is used as a first order estimate for risk assessment.

The rock mass is treated as homogeneous and the effect of natural fractures on fluid flow is represented through an overall leak-off mechanism. In the case of hydraulic fracturing treatments carried out under field conditions, it has been found that fracture propagation is dominated by viscous dissipation (Adachi et al. 2007). Therefore, in the current study, hydraulic fracture propagation is considered to be viscosity dominated (zero toughness solution).

4.3 Wellbore delamination model

The interface debonding model from Lecampion et al. (2013) has been used in this study to simulate the vertical propagation of a micro-annulus driven by constant pressure fluid injection at the inlet.

The model accounts for the buoyancy forces caused by the difference in fluid densities, the casing stiffness, and the viscous forces due to fluid flow. The model assumes a constant arc-length for the micro-annulus and can predict the width and length of the debonding, the fluid flux entering the micro-annulus, and pressure distribution within the micro-annulus as a function of time.

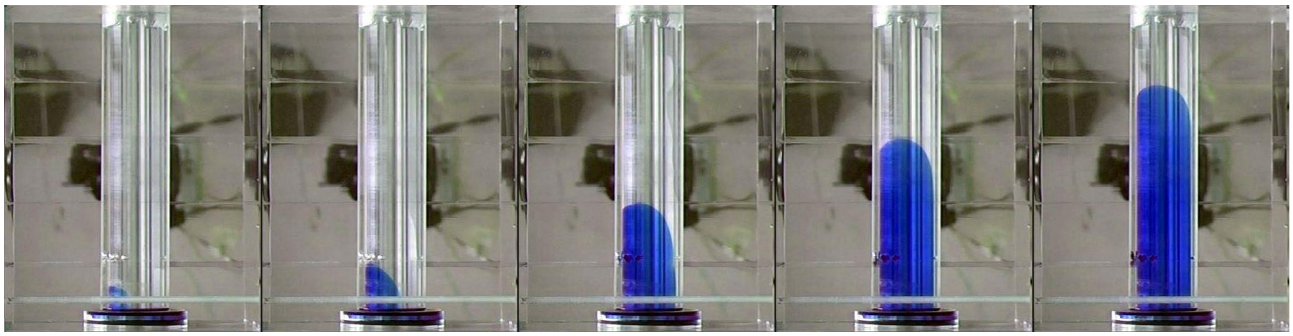

Figure 14 - Laboratory experiments designed to validate the model of micro-annulus growth. (Bunger et al. 2010)

The wellbore delamination model is based on the following assumptions: the gradient of the clamping stress is assumed to uniform along the casing/cement interface, that a defects exists around the perforations, the arc-length of the micro-annulus remains constant as it propagates upward, the injected fluid is Newtonian fluid, the toughness of the cement interface is negligible, and there are no phase changes or thermal effects (Lecampion et al. 2013). The predictions of the Lecampion et al. (2013) model of micro-annulus growth were tested with a series of laboratory experiments (Figure 14). The model approach is briefly presented in Appendix B while a detailed formulation of the method can be found in the work by Lecampion et al. (2013).

The current study only considers the propagation of the micro-annulus under constant injection pressure. However, well integrity can also be compromised by insufficient cement coverage, degradation of cement sheath and cement bonds due to cyclic stress and temperatures changes in the well, or corrosive environment, which are not considered in this study. Therefore, the results should only be used as an estimate to evaluate the potential for contamination from planned or existing wells, and a detailed site specific studies should be completed if needed.

5 Input data

This section provides a critical summary of the data collected from the two case study regions in QLD and NSW. Input data for the Surat Basin includes data from hydraulic fracturing treatments/trials carried by QGC Shell at one of their wells in the region, and for the Sydney basin in NSW, publically available data is used from the Camden Gas project (AGL 2013).

The uncertainty in the parameter values are represented using *p-box*es that enclose the cumulative distribution function (CDF) of the parameter. When calculating distribution free *p-box*es the lower and upper estimate bounds can be improved by including additional statistics such as minimum, maximum, median or standard deviation. Wherever possible these additional statistics have been added based on the data collected.

5.1 Reservoir properties and fracture treatment data

The Surat basin is comprised of various layers of sandstone, siltstone, interspersed by coal seams, with layers of volcanic rock and alluvial deposits above. In order to numerically simulate rock behaviour during different stages of drilling, completion and production, engineers often use a mechanical earth model (MEM) of the region that contains geo-mechanical information such as the mechanical properties of rock, the state of stress, and the pressure and temperature at different depths. These data are compiled from well test data, seismic surveys, and down hole logging. Table 4 summarizes key information regarding the geological layers used in the MEM of the region. It can be observed that most layers have small thicknesses averaging less than 3m and most of the coal seams are found at depth ranging from 300-600m.

The target coal in the Surat basin is the Walloon Coal Measures, it includes the upper Juandah and the lower Taroom Coal seams separated by the Tangalooma sandstone (Department of Natural Resources and Mines 2017c). The coal seams in the Surat basin are spread across multiple layers and are also of smaller thickness (0.4m) (Pandey et al. 2017). Table 5 show the cumulative coal thickness of Walloon Coal Measures across the Surat basin which ranges from 2m in the Gwydir region to a maximum of 30m in the Maranoa-Baloone-region (Pinetown et al. 2014). The height h_f in the PKN model typically corresponds to the height of the pay-zone that is to be hydraulically fractured. In the case of CSG wells, it is not feasible to hydraulically fracture individual coal seam due to their smaller thickness, so the fracture treatment is designed to cover multiple seams. The height h_f, used in the PKN model corresponds to the fracture zone and not the height of individual coal seams. In recent hydraulic fracturing trials carried out in the Surat basins, results from microseismic monitoring show that the height of the fracture zone varies between 40-110m with an average height of 61m (Pandey et al. 2017). Therefore, for the current study we assume the pay-zone height to be a non-parametric distribution with an average height of 60m, with a minimum and maximum values of 40 and 70m respectively.

Table 4 - Surat basin average thicknesses for coal, sand, shale and siderite.

Formation type	No. of layers between 100-300m	Average thickness(m)	No. of layers between 300-500m	Average thickness(m)	No. of layers between 500-600m	Average thickness(m)	No. of layers between 600-725m	Average thickness(m)
Coal	04	2.14	40	0.79	28	0.63	15	1.29
Sand	151	0.73	139	0.51	108	0.31	72	0.50
Shale	157	0.42	188	0.46	140	0.32	97	0.43
Siderite	02	0.18	13	0.83	16	0.33	15	1.47

Table 5 - Thickness of coal seam across the Surat basin.

Formation	Location	Average thickness (m)	References
Taroom Coal	Surat	08	QGC Limited (2009)
	Hopeland, Surat	06	
Juandah Coal	Surat	22	Draper and Boreham (2006); Papendick et al. (2011); Geoscience Australia and Australian Stratigraphy Commission (2017)
	Hopeland, Surat	16	
	Dalby, Roma	3-4	
Cumulative Walloon Coal Measures	Gwydir	2	Pinetown et al. (2014), Scott (2008)
	Maranoa-Baloone-Condamine	30	

The depth of hydraulic fractures (or the injection depth) was assigned a non-parametric distribution with a mean of 520m, a minimum of 400 m and a maximum of 800m, based on some of the recent hydraulic fracturing trials carried out in the Surat basin (Pandey et al. 2017), and the information supplied by QGC. A minimum injection depth of 400m is assumed and justified based on the stress regime in the Surat basin. For depths shallower than 400m the vertical stress is the minimum principal stress (Flottman et al. 2013). As hydraulic fractures grow in a direction perpendicular to the minimum principal stress, for depths less than 400m fracture propagation would be predominantly horizontal. Horizontal fractures contribute little towards increasing the production from the reservoir and higher permeability at shallow depth make hydraulic fracturing unnecessary, (Valkó and Michael J. 1995).

The Bulli and Balgownie coal seams in the Illawara Coal measures in the Sydney region, are located between depths of 640-700m (AGL 2013). The average depth of The Bulli and Balgownie coal seams are 666m and 683m respectively. Therefore, for the Sydney region, the injection depth was assigned a non-parametric distribution with upper and lower bounds of 640 and 700m respectively, with a mean depth of 675m.

A data set supplied by QGC from a hydraulic fracturing trial was used in this study. The fracture treatment parameters used are a combination of values reported in literature and based on QGC data. Non-parametric distributions are assigned a range (minimum and maximum) based on values reported in literature, and a mean value based on the data set supplied by QGC.

The injection rate is one of the important factors that determine the size of hydraulic fractures. In the design phase of the fracture treatment, the injection rate is calculated after taking into consideration the number of stages, the number of fractures per stage, maximum pump rate and the allowable pressures on the wellhead and the casings. Higher injection rates reduce the effects of fluid loss to the surrounding rock. Kirk-Burnnand et al. (2015) carried out a study in the Surat basin, and based on the tiltmeter surveys found that all hydraulic fractures generated during the treatment had a horizontal and vertical component, but the horizontal component was higher for treatments carried out using higher pumping rates. Based on these findings, they recommend using lower pumping rates as the best approach to obtain vertical hydraulic fracture growth. So for the current study, an injection rate Q in the interval 0.96-3.2 $\mathrm{m}^3/\mathrm{min}$ with a mean of 1.6 $\mathrm{m}^3/\mathrm{min}$ is used based on supplied QGC data set.

The stimulation efficiency η is the ratio of the total fluid volume minus the loss into the surrounding rock compared to the total fluid injection. CSIRO has used hydraulic fracturing to precondition rock in underground mines to improve safety and production (Jeffrey, R.G. et al. 2013). CSIRO monitored the operations with an array of measuring devices showing that treatment efficiencies were between 40 and 60% around 300m (Chen and Jeffrey 2009). In the case of CSG wells, coal seams contain natural fractures or cleats, meaning that a large proportion of injected fluid can be lost in the formation (Li et al. 2015). Therefore, the treatment efficiency for this study is assumed to between 30-50% with mean value of 40%. Leak-off is included in the PKN model by using the treatment efficiency to obtain an effective injection rate $Q^* = \eta Q$.

The average injection time t used is 30 min with the minimum of 20 min based on the data supplied by QGC and, the maximum injection time used is 120 min based on literature data. The injection pressure during the fracturing trial conducted by QGC was around 11.7 MPa, and Pandey et al. (2017) report that fracturing treatments carried out in the Surat basin show an injection pressure of around 15.5 MPa. Based on these values, an injection pressure between 10 and 20 MPa, with an average of 12MPa is used for this study. During the injection phase, the pressure acting on the well casing is estimated from the injection pressure and once the well is decommissioned the pressure acting on the well casing is taken as the hydrostatic pressure at that depth. Using hydrostatic pressure during decommissioning is based on the assumption that the wellbore fills up with water after decommissioning, additionally, any buoyancy effects are not included in the model in this study.

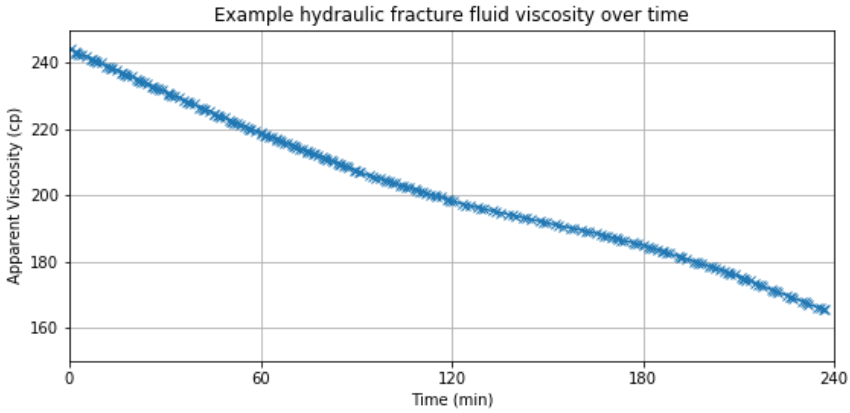

Figure 15 - Hydraulic fracturing fluid viscosity measure with time for typical CSG hydraulic fracturing.

Fracturing fluids are mostly water based fluids whose viscosity is modified using additives such as guar or potassium chloride. The choice of additive and proppant depends on the treatment design and the formation characteristics. The QGC study used a borate crosslinked gel whose viscosity varies with time as shown in Figure 15. Based on the figure and using the values for the injection times, the average viscosity of the injected fluid μ was set as 230cp with a range between 200-235cp.

The fluid leaking through the micro annulus is taken to be the fracturing fluid in the fracturing phase and the formation fluid (water) after the well is decommissioned. As the fracturing fluid is predominantly water its density is assumed to 1000 kg/m^3. The data collected for the Surat basin by QGC shows that the horizontal stress gradient in the region ranges from 14.7-18.1 kPa/m. The vertical stress gradient used is 22.6 kPa/m and hydrostatic pressure gradients is taken as 9.726 kPa/m (Kirk-Burnnand et al. 2015).

As per the code of practice for the construction and abandonment of CSG well in Queensland, the following casing dimensions are commonly used by the CSG industry: 9-5/8” (245mm) casing in 12-1/4” (311mm) hole, 7” casing (178mm) in 8-1/2” (216mm) hole and 5-1/2 (140mm)” casing in 7-7/8 (200mm)’’ hole (Department of Natural Resources and Mines 2017d). To estimate typical casing dimensions used in CSG development, data was compiled from well completion reports submitted by different companies involved in CSG development in Australia, from the well completion reports database maintained by Queensland and NSW, and the code of practice guide for CSG wells published by NSW and QLD (Department of Industry NSW 1998; Department of Natural Resources and Mines 2017d; Department of Trade and Investment, NSW 2012; Bioregional Assessment Source Dataset 2014; Geoscience Information of Geological Survey of Queensland 2016). Casing dimension of 5-1/2” and 7” was most commonly used across all the data sources. Therefore the analysis was carried out for these casing dimensions. Class G cement is most commonly used for well cementing in the oil and gas industry (Guner et al. 2017). For this study we assume Class G cement with an Young’s modulus and Poisson’s ratio of 8GPa and 0.15 respectively (Lecampion et al. 2013).

Table 6 - Mechanics properties for coal and rock layers, cement and well casing.

Component	Symbol	Young's Modulus (GPa)	Poisson's Ratio	Reference
Shale	E_3	28	0.14	Pollard and Fletcher (2005)
Sandstone	E_3	22	0.24	Pollard and Fletcher (2005)
Coal	E_3	Minmaxmean (2.6,3.4,2.9)	0.35	Pandey et al. (2017)
Cement	E_2	8	0.15	Guner et al. (2017), Lecampion et al. (2013)
Casing	E_1	200	0.3	Standard values for steel

The formation consists of layers of shale, sandstone, coal each having different mechanical properties as summarized in Table 6. As the hydraulic fracture and wellbore delamination models consider the rock to be a homogeneous medium, we use the equivalent/averaged properties E^* and ν^* which are defined as

$$\mathrm{E}^* = \sum E.h / \sum h \qquad \nu^* = \sum \nu.h / \sum h \tag{3}$$

where E and h are the Young's modulus and thickness of individual layers respectively, in the mechanical earth model. For the CSG wells in the NSW, the mechanical earth model is not available, so we assume an average modulus and Poisson's ration of reservoir rock to be 20 GPa and 0.2 respectively. The Young's modulus of coal is set at an average values of 2.9 GP within the range of 2.6-3.4 GPa, and a Poisson's ratio of 0.35 based on the hydraulic fracturing case studies carried out in the Surat basin (Pandey et al. 2017).

Data and variables used in the mathematical model to determine probability estimates are listed in Table 7.

Table 7 - Data used in the hydraulic fracturing and wellbore delamination probability bounds analysis.

Parameter	Symbol	Value/*P-box*	Reference
Injection rate $\mathbf{m^3/min}$	Q	Minmaxmean (0.96, 3.2, 1.6)	Pandey and Agreda (2014; Kirk-Burnnand et al. (2015)
Viscosity of injected fluid (cp)	μ	Minmaxmean (200, 235, 230)	QGC data
Total injection time (min)	t	Minmaxmean (20, 120, 30)	QGC data, Pandey et al. (2017)
Treatment efficiency	η	Minmaxmean (0.3, 0.5, 0.4)	Chen and Jeffrey (2009)
Density of fluid (water) leaking through the micro annulus	ρ	1000 kg/m^3	Density of water
Vertical stress gradient (kPa/m)	σ_v	22.62	Kirk-Burnnand et al. (2015)
Reservoir pore pressure (kPa/m)	p	9.78	Hydrostatic gradient
Horizontal stress gradient (kPa/m)	σ_H	14.7-18.1	QGC data
Injection depth (m)	D	Minmaxmean (400,700,520)	Flottman et al. (2013); Department of Natural Resources and Mines (2017), QGC data
Height of pay zone (m)	h_f	Minmax(40,70)	Pinetown et al. (2014)
Casing diameter (mm)	$2R_1$	140, 178	Department of Natural Resources and Mines (2017d)
Well diameter (mm)	$2R_3$	200, 216	

5.2 Separation distance to Aquifer and water bores

5.2.1 Sydney basin (Camden region)

This study uses publically available data from the Camden region in NSW published by AGL (AGL 2013). The major aquifers/water bearing zones in the Camden region are Quaternary and Tertiary alluvial/sediments, the Wianamatta system, Hawkesbury Sandstone, the Narrabeen Group sandstone aquifers and the Permian water bearing zones.

The aquifer types in these stratigraphic units, their hydrogeological properties and information about the number of water bores that tap water from these systems are summarized in Table 8. The alluvial deposits and the Hawkesbury Sandstone together form the major aquifer systems, with most of the water bores concentrated in these stratigraphic layers. The alluvial aquifers are more localized than the Hawkesbury sandstone that cover almost the entire region of the Sydney basin. The AGL report, for example, has provided consolidated information about 113 licensed water bores in the Camden region collected from the Pinneena database (NSW ground water data archive 2010). Seventy eight of these wells tap water from the alluvial aquifers and the Hawkesbury sandstone, for irrigation, livestock and domestic needs. The water bores in the unconsolidated sediments or alluvial deposits are less than 30m deep, while the water bores in the Hawkesbury Sandstone are between 100-300m deep (relative from the ground surface). For water contamination the vertical separation distance between the between the deepest water bore and the shallowest targeted coal seam is the most important aspect. Comparing well depths to the Illawarra coal measures coal seam results in an average minimum separation distance of 340m.

Table 8 - Hydrogeological properties of stratigraphic units in the Camden region
Source: AGL (2013)

Aquifer	Aquifer type	Water Quality	Yield (L/s)	No. of water bores	Depth below ground level
Quaternary and Tertiary alluvial deposits	Beneficial Aquifer	Good/Excellent	2.6	33	5.6#
Wianamatta Group aquifers	Aquitards/ small aquifers	Fresh to Brackish	1.3	12	3.5#
Bald Hill Claystone Aquitard – 34m thick					
Hawkesbury Sandstone aquifer system	Major aquifer	Fresh	2-40	45	43#
Stanwell Park Claystone Aquitard – 36m thick					
Narrabeen Group sandstone aquifer (Bulgo sandstone and Scarborough sandstone)	Minor non-beneficial aquifers	Poor	0.2-2	0	274-636
Wombarra Claystone Aquitard – 32m thick					
Permian water bearing zones – Illawarra coal measures	Minor water bearing zones	Very Poor	-	0	667-699

- Average standing water level.

5.2.2 Surat Basin

The major aquifers in the Surat Basin are the Bungil Formation, Mooga, Gubberamunda, Springbok, Hutton and the Precipice Sandstones (QWC, 2012), and the major aquitards include the Evergreen, Birkhead, Westbourne, Orallo, Wallumbilla and Griman Creek Formations. Shallow aquifers used by regional communities include the Condamine Alluvium and Main Range Volcanics, while the sandstone aquifers are less developed (Department of Natural Resources and Mines 2016). Table 9 provides a summary of the aquifer types in the stratigraphic units across the Surat basin, their hydrogeological properties and statistics on the number of water bores that source water from these aquifers. The Condamine Alluvium is a major source of water in the region with an estimated 64,000 mega litres extracted annually. Some water bores targeting the Condamine Alluvium were drilled into the top of the Walloon Coal Measures because it is often difficult to distinguish the weathered upper bedrock from a layer of alluvial clay (Department of Natural Resources and Mines 2016).

The upper and lower Walloon coal measures (WCM), are technically aquitards but are not as thick as the Westbourne or other aquitards. The water quality in the WCM is generally poor, but at shallow depth the water quality is better and is used by the local community (Department of Natural Resources and Mines 2016). The water quality in the Springbok aquifer is highly variable. At some locations it is an important aquifer but in other places it is highly compacted and has very low permeability. The separation distance between the coal measures and the beneficial aquifers varies across the region. The Gubberamunda sandstone for example is separated by 65m to 200m from WCM, while the Hutton is 150 to 350m from WCM.

Table 9 - Hydrogeological properties of stratigraphic units in the Surat region

Source: Department of Natural Resources and Mines (2016); Department of Natural Resources, Mines and Energy (2017b)

Aquifer	Aquifer type	Water Quality	Yield (ML/year)	No. of water bores	Depth below ground level
Condamine River Alluvium	Beneficial Aquifer	Excellent	72,024	3853	0-40
Other Alluvium	Beneficial Aquifer	Excellent		1523	
Gubberamunda Sandstone	Artesian aquifer		4,662	561	
Westbourne Formation Aquitard – 100m thick (where present)					
Springbok Sandstone		Poor (west Surat) – Okay (eastern Surat)	4,337	265	170-1500
Waloon Coal measures (upper aquitard)					
Walloon coal measures	Minor water bearing zone		1,647	11,418	200-1700
Walloon Coal measures (lower aquitard)					
Durabilla/Eurombah Formation	Minor water bearing zone		281	443	500-2000
Hutton Sandstone	Major Aquifer		14,983	2,645	500-2000

- Average standing water level.

6 Results and discussion

The following sections (6.1 and 6.2) provide a summary of the findings from this study. The results are presented in the form of *p-boxes* which shows the bounds on the cumulative distribution function (CDF) under a *best* and *worst* case scenarios. *Best and worst* are the boundaries of the scenarios and do not imply either good or bad. For example, maximizing the fracture length within the pay-zone would increase production and reduce the number of wells required (good), conversely, a shorter fracture length and height reduces the distance to aquifers and water bodies (also good).

6.1 Hydraulic fracture model

The hydraulic fracturing model was calculated for the Surat basin only. Figure 16 shows the p-box generated for the hydraulic fracturing study based on the variable ranges listed in Table 7 for the Surat basin. The *x-axis* corresponds to the fracture half-length in metres computed using the PKN model discussed in section 4.2, and the *y*-axis represents the cumulative probability for the fracture half-length to take a specific value.

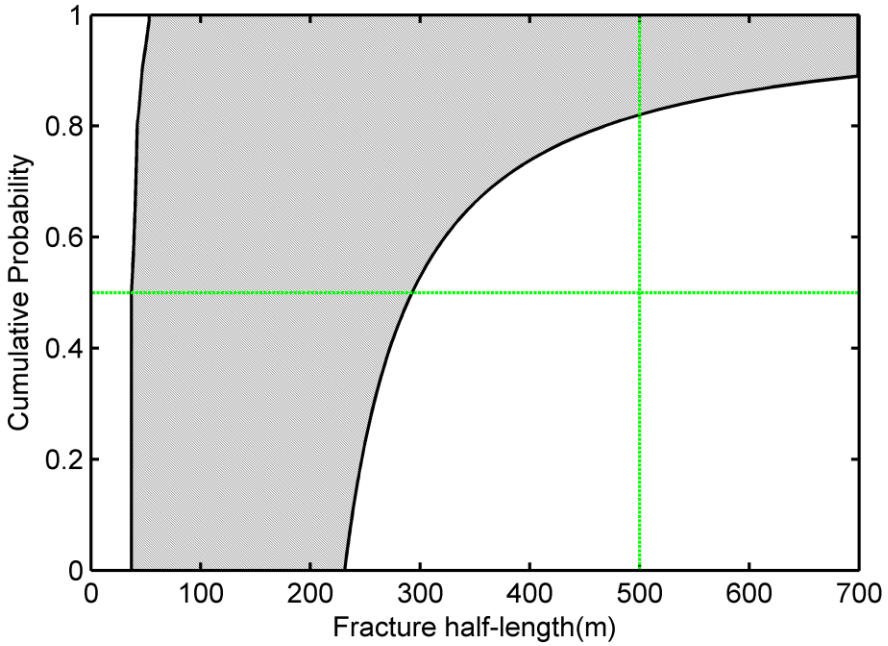

Figure 16 - *P-box* for the fracture half-length – PKN model. (green lines 50th percentile, 80th percentile less than 500m)

The cumulative distribution function (CDF) of the fracture half-length is unknown but is bounded by the *p-box*. Any and all CDFs within the p-box are possible (See Appendix C: Probability box for further examples). The left and right side of *p-box* shows the smallest and largest possible half-lengths which are not exceeded under shortest and longest fracture half-length scenarios respectively. For example, the 50th percentile values for the fracture half-length is between 37m and 291m.

The minimum probability that the fracture length is less than 500m is 83%. Table 10 shows the 50th percentile values for the fracture length, the wellbore opening, and the net pressure obtained using the PKN model. The net pressure from the model can be used to indirectly verify the calculation as the sum of net pressure and the far-field confining stress should roughly equal the bottom hole pressure or the sum of surface pressure and hydrostatic head. The difference between the minimum and maximum values represents the uncertainty based on the region wide data. Similarly, the *p-box* for the fracture height predicted using the radial (penny shaped) model is shown in Figure 17, and the 50th percentile values for the fracture radius and the opening are summarized in Table 11.

Table 10 - Hydraulic fracturing risk computed using the PKN model.

Parameter	50th percentile - Min	50th percentile - Max	Uncertainty
Fracture half length(m)	37	291	254
Fracture opening (mm)	2.9	7.3	4.5
Net pressure (MPa)	1.0	4.3	3.3

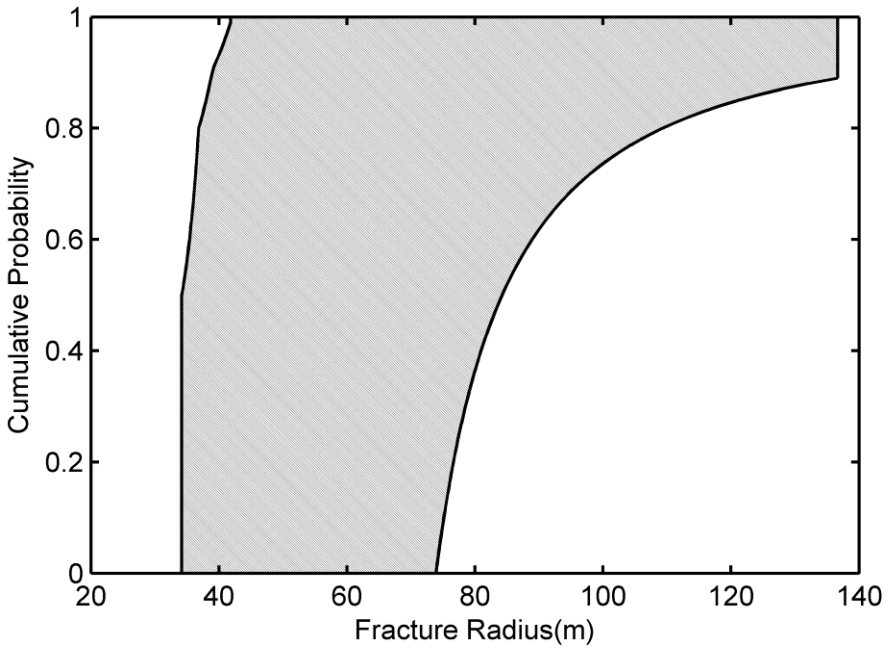

Figure 17 - *P-box* for the fracture radius using the Penny shaped model.

Table 11 - Maximum height growth – Penny shaped model

Parameter	50th percentile - Min	50th percentile - Max	Uncertainty
Fracture radius / height (m)	34	84	50
Fracture opening (mm)	2.9	5.5	2.6

The use of the PKN model provides a conservative estimate for the lateral extent of the fracture while the radial model provides a conservative estimate for the height. The worst case 99.9th percentile values for the fracture half-length and the fracture height/radius were 699m and 137m

respectively. *However, these numbers should not be taken as an exact measure of the maximum fracture length or the height under field conditions.* These values are conservative estimate based on the basin wide data. The results should not be interpreted that all fractures would or would not interact with an aquifer. Not all CSG wells are in regions where the separation distances are small, and not all CSG wells are hydraulically fractured. There are also additional factors such as stress regimes that vary with depth, stresses in bounding rock layers, etc., that limit height growth. Furthermore, fracture growth during hydraulic fracture operations are monitored and fracture growth is suspended or halted when conditions indicate that pressure cannot be maintained in wells.

For this study we have used information related to the fracture treatment that was available for the Surat basin. Although the data is generally representative of the Surat basin, it should be noted that the basin covers a large geographical area and varies significantly. Additional site specific information would reduce the uncertainty in the input data and tighten the bounds on the model output. In the absence of specific information on the degree of correlation between input variables, this analysis assumes that the input variables are independent therefore the results are conservative.

Hydraulic fracture half-length and height can be visualised by combining data from the p-box output. Representation of 50th, 75th, 80th and 99.99 percentiles is shown in Figure 18. The width and height of percentile box represents uncertainties of fracture length and fracture radius/height respectively. The uncertainty (box area) is dependent on size of region studied and possible hydraulic fracture treatment parameters, this uncertainty magnitude decreases as site specific information is added meaning that risks associated with any individual hydraulic fracturing operation are minimised especially when they are conducted within regulations defined by broad area analyses.

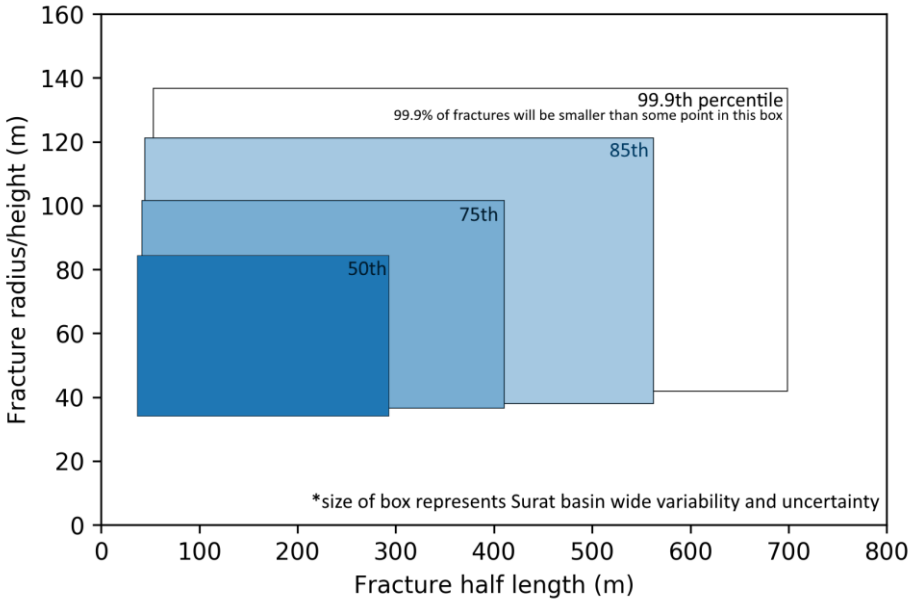

Figure 18 - Representation of the 50, 75, 80 and 100 percentile values for fracture half length and height. The size of the box represents the magnitude of the epistemic uncertainty.

The fracture half-length and the fracture height estimates can be used to define an approximate "zone of influence" at different probability levels. This zone of influence can useful to define an area

nearby to existing well or aquifer that could be impacted by a hydraulic fracture treatment. For example, if the fracture length must be shorter than a certain length to minimize the risk of interaction with a nearby wellbore, the length likelihood can be referenced from the *p-box* and used as a setback distance more generally, thereby ensuring minimal residual risk.

An example of adding specific hydraulic fracturing treatment data to the PBA model is shown in Figure 19 where Example Scenario A corresponds to a subset of the input data from Table 12. As can be observed the additional information reduces the uncertainty of the 99.9th percentile fracture length from 646m to 223 m, and fracture radius/height from 95 m to 40 m.

Table 12 – Parameters used for Example Scenario A PBA analysis, only hydraulic fracturing input data that differs to input data in Table 7 is shown.

Parameter	Example Scenario A	Basin wide data (Table 7)
Injection rate $\mathbf{m^3/min}$	Minmaxmean (0.96, 2.0, 1.6)	Minmaxmean (0.96, 3.2, 1.6)
Total injection time (min)	Minmaxmean (20, 60, 30)	Minmaxmean (20, 120, 30)
Height of pay zone (m)	40	Minmax(40,70)

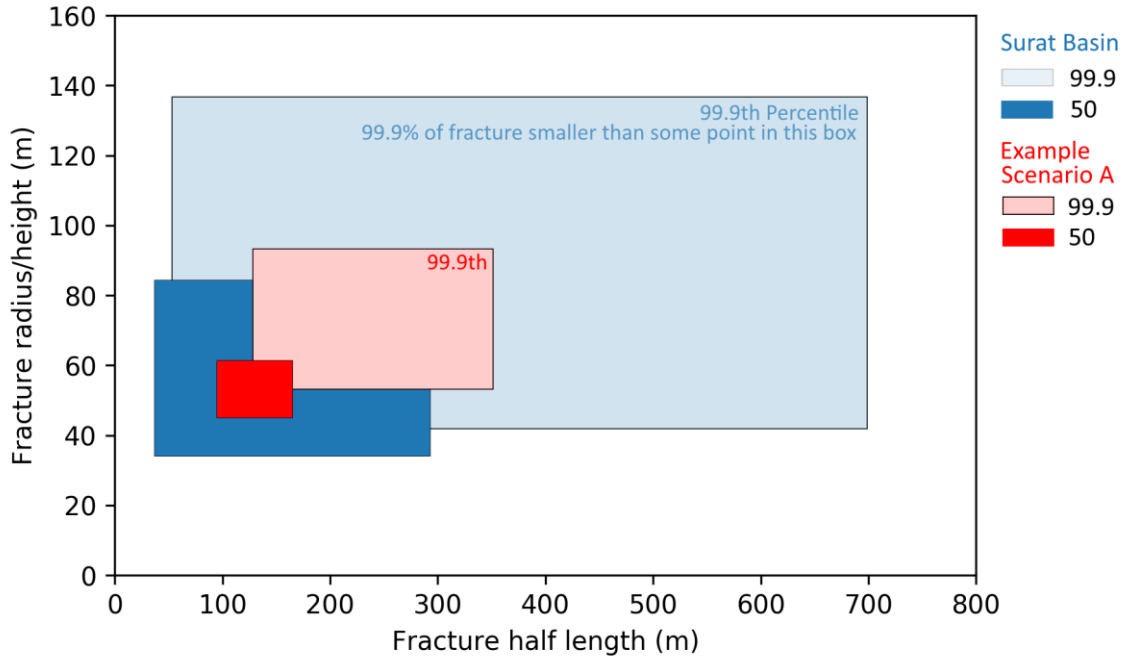

Figure 19 - Example Scenario A with more informed dataset overlayed on basin wide dataset. Example Scenario A's 99.9th and 50th percentile show reduced uncertainty (area of box) when compared to basin wide information.

6.2 Wellbore delamination model

The risk of a micro-annulus creating a delaminated wellbore fluid flow pathway which may interconnect different geological layers was calculated both for the Surat and the Sydney basins. As mentioned in Section 5.1, casing dimensions of 5-1/2" (140mm) and 7" (178mm) are commonly used in CSG well across Australia. Therefore, the study was conducted for both these dimensions.

As introduced in Section 2.2.1, potential micro-annulus growth in two different phases of the well life cycle have been investigated: during hydraulic fracturing and post decommissioning after the end of the production. During the production phase, the pressure in the wellbore is maintained below the reservoir pressure to enable the methane gas in the coal seam to flow into the wellbore, which implies that there is a lower driving force available to propagate a micro-annulus up the wellbore.

6.2.1 Micro-annulus growth during hydraulic fracturing

Figure 20 shows the p-box generated for the micro-annulus (crack) length during the hydraulic fracturing phase in the Surat basin for two different casing diameters, and the 50th percentile values for the fracture radius, the crack opening, and the fluid volume entering the micro-annulus are summarized in Table 13.

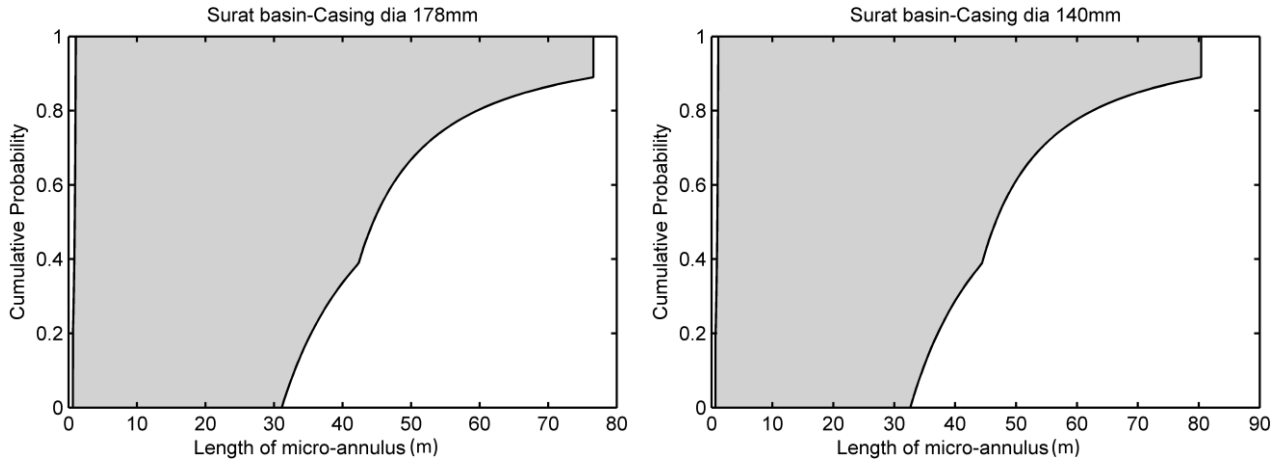

Figure 20 - *P-box* for the length of the micro-annulus in the Surat basin for two different casing diameters: 178mm (left) and 140mm (right).

Table 13 - Wellbore delamination risk during the Hydraulic fracturing in the Surat Basin (50th percentile values)

Parameter	Casing dimeter – 178 mm			Casing dimeter – 140 mm		
	Min	Max	uncertainty	Min	Max	uncertainty
Length of Micro-annulus (crack) (m)	1	44	43	1	46	45
Fracture Opening (Microns)	52	72	20	50	70	20
Fluid volume entering the micro-annulus during hydraulic fracturing (litres)	0.02	0.18	0.16	0.01	0.15	0.14

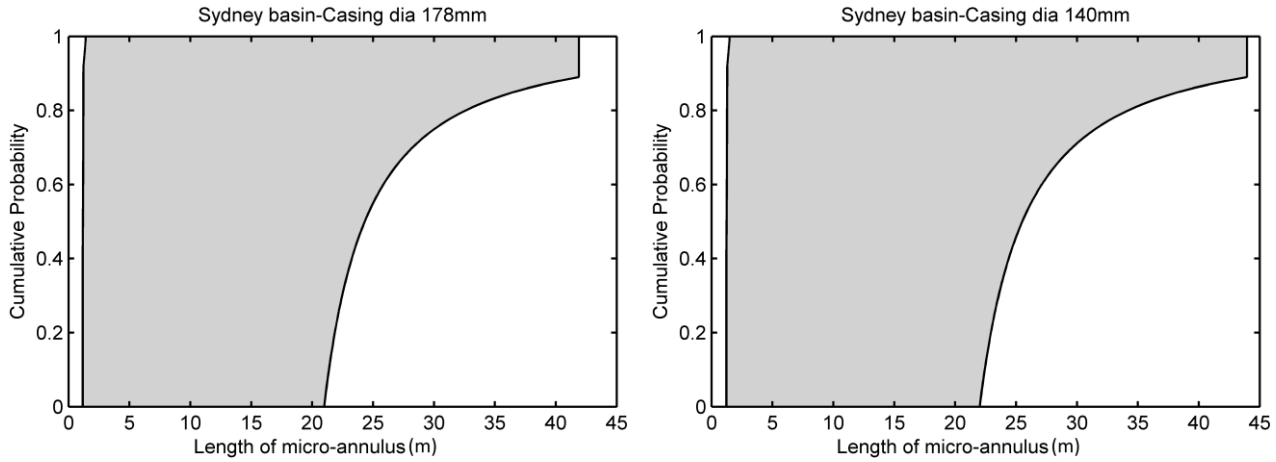

Figure 21 - *P-box* for the length of the micro-annulus in the Sydney basin for two different casing diameters: 178mm (left) and 140mm (right).

The 99.9th percentile values for the length of the micro-annulus for casing dimensions of 178mm and 140mm were around 77m and 80m respectively, but the 50th percentile values were less than 50m. The *p-box* generated for the micro-annulus (crack) length in the Sydney basin is shown in Figure 21 and 50th percentile values for crack length, opening and fluid volume entering the micro-annuli are summarized in Table 14.

Table 14 - Wellbore delamination risk during the Hydraulic fracturing in the Sydney Basin (50th percentile values)

Parameter	Casing dimeter – 178 mm			Casing dimeter – 140 mm		
	Min	Max	uncertainty	Min	Max	uncertainty
Length of Micro-annulus (crack) (m)	2	24	22	2	25	23
Fracture opening (µm)	52	104	52	50	100	50
Total fluid volume entering the micro-annulus during hydraulic fracturing (litres)	0.02	0.30	0.28	0.01	0.25	0.24

It can be observed from Table 13 and Table 14 that the length of micro-annulus predicted for the Surat basin has a higher uncertainty than the corresponding values for the Sydney basin, which is due to uncertainty in the input data. In the case of the Sydney basin the depth of the Illawara Coal measures is fairly uniform between 640-700m, while for the Surat basin the depth can vary greatly, which make it difficult to define a tighter range for the injection depth. But it can be noted that the 50th percentile values for the micro-annulus length is less than 50m in both cases. In the case of Sydney basin the minimum distance to an overlying aquifer is greater than 340m (Section 5.2.1) therefore is of minimal concern. In the case of the Surat basin, for hydraulically fractured well we have assumed the height of pay-zone as 40-70m and in a worst-case scenario, the annulus crack is likely to be about the size of the pay-zone. Considering that the fracturing depth is likely to be more than 400m, it is unlikely that the micro-annulus would reach an overlying aquifer. It is evident from Table 13 and Table 14 that in any scenario the micro-annulus opening is less than 100 µm and the resulting fluid volume entering the micro-annuli is less than 0.3L. To put that into perspective the thickness is equivalent to an 80 gsm copying paper and the fluid volume entering the annulus crack

is equivalent to a can of drink. Therefore, it is reasonable to assume that interface debonding will not result in any significant contamination during the hydraulic fracturing phase.

6.2.2 Micro-annulus growth post decommissioning

Both QLD and NSW governments have a code of practice that must be followed for decommissioning of CSG wells and other drill holes at the end of their production life to ensure well isolation and the protection of groundwater resources (Department of Natural Resources and Mines 2017d; Department of Trade and Investment, NSW 2012). During the post-decommissioning phase, it is only the local bottom hole fluid pressure that drives the micro-annulus growth. Formation fluid flowing into the micro-annulus is assumed to have a viscosity of 1 cp. During decommissioning, the steel casing is filled with cement to isolate different sections of the formation, and prevent migration of fluid. To arrive at a conservative estimate it is assumed that the steel casing is filled with water (rather than cement) and the pressure is hydrostatic.

Model and input parameters have been chosen such that in this scenario the micro-annulus will reach the surface. This allows us to determine the width of potential micro-annuli and assess the risk profile of this pathway. In practice, this situation would never occur and a properly designed well completion contributes to negative buoyancy in the micro-annuli that arrests vertical propagation in the micro-annulus (Lecampion et al. 2013).

Figure 22, shows the time it would take for a micro-annulus to reach the surface where the driving pressure is hydrostatic in the Surat and Sydney basins. In the decommissioning phase the only parameter that is uncertain is the well depth which influences the hydrostatic pressure.

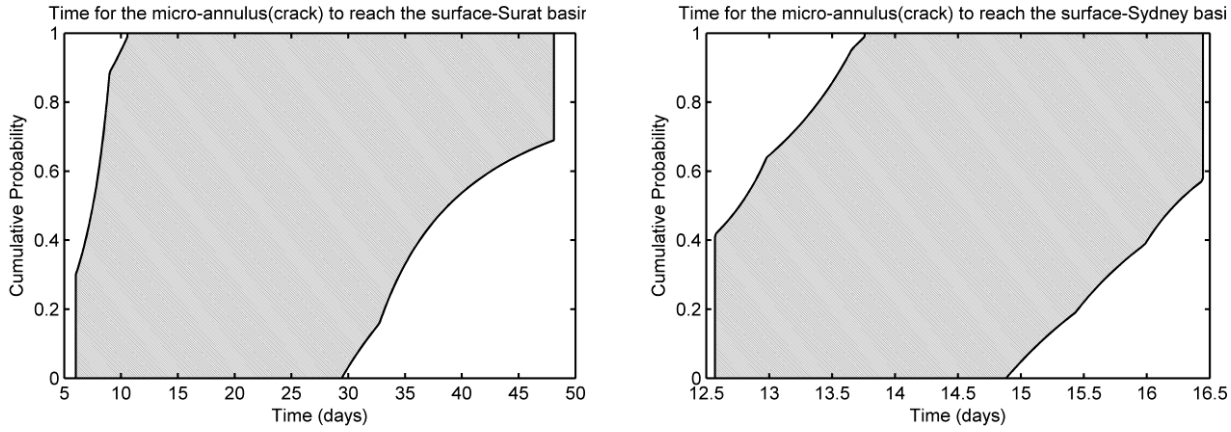

Figure 22 - *P-box* for the risk due to wellbore delamination after the well is decommissioned showing the time it would take for the micro-annulus crack to reach the surface for the Surat Basin (Left) and the Sydney Basin (Right)

The 50th percentile values in Table 15 show that the time taken for the micro-annulus to reach the surface is less than a month. The opening of the micro-annulus predicted by the model is less than 50 µm. The flux through the micro-annulus will be sustained while there is positive pressure. The hydrostatic pressure, which is the main driving force, decreases as the micro-annulus propagates upwards. When the micro-annulus reaches the water table level or a height where the pressure is atmospheric, there is no further driving force and the propagation arrests. Fluid flow out of the

micro-annulus at the surface is zero as there is no driving force to move the fluid. However, methane gas or other hydrocarbons could potentially bubble through the micro-annulus.

Table 15 - Wellbore delamination risk after decommissioning in the Surat Basin and Sydney basin for a casing diameter of 178mm (50th percentile values)

Parameter	Surat Basin			Sydney Basin		
	Min	Max	uncertainty	Min	Max	uncertainty
Time to reach the surface (days)	08	39	31	13	17	14
Fracture opening (µm)	20	32	12	32	35	03

The total gas volume that can flow through any given aperture depends on the pressure. During production from a CSG well, the pressure within the reservoir is reduced by pumping out the water from the wellbore which mobilises gas adsorbed in the coal matrix. After production is finished the gas mobility is reduced as the pressure near the wellbore equilibrates to the reservoir pore pressure. The simulated micro-annulus when grown to the surface was estimated to have an opening less than 50 microns and will be filled with at least water leading to the likelihood of significant gas flux through the micro-annulus to be low. While this study considers a potential leak through the micro-annulus, leaks through other mechanisms could be possible by compromised well integrity such as insufficient cement coverage or cement degradation, natural faults that connect to aquifers, or methane escaping from shallow coal seam seams. Several of these additional risks can be mitigated by compiling to the mandatory requirements outlined in the codes of practice for constructing and abandoning coal seam gas wells in Queensland and NSW (Department of Natural Resources and Mines 2017d; Department of Trade and Investment, NSW 2012), running independent cement bond logging and completing sufficient subsurface area characterisation.

7 Conclusions

In this study, hydraulic fracture propagation and wellbore delamination models were used with basin scale data, and probability bound analysis to determine the likelihood of surface and groundwater contamination due to unconventional gas development in the Surat and Sydney basins. Both the hydraulic fracturing and wellbore delamination models chosen are conservative and computationally efficient.

The estimates for hydraulic fracture dimension and associated probabilities in the form of *p-boxes* present risk on a basin scale without having to analyse individual wells or rely on qualitative risk statements. The p-box analysis is used for the following conclusions:

- The wellbore delamination model show that the risk of contamination to overlying aquifers is low for the Sydney and Surat basins.

- Post-decommissioning micro-annuli when extended to the surface were estimated to have an opening less than 50 microns with low likelihood of significant gas flux through the micro-annulus. Therefore, the potential for gas leak from a micro-annulus to the surface, if it exists, is negligible.

- The hydraulic fracturing study in the Surat basin indicated that there is an 83% likelihood for the fracture length to always be less than 500m. Additionally there is a 74% likelihood the fracture height will always be less than 100m. Considering the geological variation across the Surat basin, it is not applicable to conclude if the fractures would intersect an overlying aquifer or a wellbore. However, a future study could combine this PBA model with a grid-based spatial method to simulate all subregions.

- The uncertainty in the PBA results can be reduced by using localised data within a basin or with specific hydraulic fracture design.

The PBA method presented in this study is a framework that can be used for risk assessment studies or for the development of risk profiles for other unconventional resources such as shale gas or tight gas.

Glossary

Term	Description
Aleatoric uncertainty	Statistical uncertainty or uncertainty due to variability or known randomness. Examples include wind speeds, the flip of a coin, the rolling of dice or the response of a structure to a random ground motion. This type of uncertainty is inherent and cannot be reduced but estimates can be improved by using past data and probabilistic models.
Aquifer	An identifiable stratigraphic formation that has the potential to produce useful flows of water and may include formations where, due to hydraulic fracturing activity, a changed hydraulic conductivity allows such water flows.
Cement sheath	A cement ring in the annulus between the casing and the wellbore, or between two casing strings.
Conductive pathways Migration pathways	Pathway that may allow flow of fluid or gas from one rock formation to another formation or infrastructure. Pathways may include hydraulic fractures, wells, other boreholes, conductive faults and natural fractures.
CSG Coal seam gas	A form of natural gas typically extracted from permeable coal seams at depths of 300 to 1000 m. Also called coal seam methane (CSM) or coalbed methane (CBM). https://gisera.csiro.au/more-information/frequently-asked-questions/what-is-coal-seam-gas/
Debonding / Interface debonding	A micro-annulus along the interface between cement barrier and steel casing and/or between the cement barrier and the surrounding rock.
Drilling mud	Provides cooling and lubrication to the drill bit and drill string, lift drill cuttings from the well and is a components of well control.
Epistemic uncertainty	Epistemic uncertainty is insufficient knowledge about a system; things that could be known but are not. Common examples include mathematical models that neglect certain effects to obtain simple closed form solutions. These types of uncertainty do not exist in nature and can be reduced with better understanding of the system. For example, when considering acceleration due to gravity the air resistance is ignored for simplicity. This epistemic uncertainty can be reduced by

	considering a mathematical model that accounts for air resistance.
Formation fluid	Any fluid within the pores of the rock. May be water, oil, gas or a mixture. Formation water in shallow aquifers can be fresh. Formation water in deeper layers of rock is typically saline.
Geogenic	A naturally-occurring chemical originating, for example, from geological formations
Groundwater	Water occurring naturally below ground level (whether in an aquifer or other low-permeability material), or water occurring at a place below ground that has been pumped, diverted or released to that place for storage. Does not include water held in underground tanks, pipes or other works.
Hydraulic Fracturing	Also known as 'fracking' or 'fraccing', involves the injection of a fracturing fluid into a target formation in order to increase the permeability of the formation and allow extraction of hydrocarbons. The wellbore casing in the zone to be fractured is perforated and then isolated using mechanical plugs or other devices, before the hydraulic fracturing fluid is injected into the isolated wellbore zone. Hydraulic fracturing fluid is pumped into the isolated wellbore zone until pressure exceeds a threshold known as the breakdown pressure. Once the hydraulic fracture fluid pressure exceeds the breakdown pressure it fractures the rock resulting in *hydraulic* fractures or reopens existing fractures.
In-situ stress	The stress acting on the rock
Leak-off	The process that results in fluid lost during a hydraulic fracture treatment by diffusion from the fracture into the surrounding rock.
Likelihood	The chance of something occurring given specific observed data.
Micro-annuli	Gap/crack created by debonding of the cement/casing or cement/rock interfaces
Minimal principal stress	The state of stress in the earth is completely described by three mutually perpendicular normal stresses. The least of these three stresses is the Minimal principal stress. Hydraulic fractures orient themselves as a plane perpendicular to the minimum principal stress.
Overburden	Material of any nature, consolidated or unconsolidated, that overlies a deposit of useful materials such as ores or coal, especially those deposits that are mined from the surface by open-cut methods.

Pay-zone	The rock layer or layers containing hydrocarbons and that is the intended zone targeted for hydraulic fracture stimulation.
Permeability	The measure of the ability of a rock, soil or sediment to yield or transmit a fluid. The magnitude of permeability depends largely on the porosity and the interconnectivity of pores and spaces in the ground.
Pore pressure	The pressure of formation fluids in pores within rock in the subsurface.
Probability bound analysis (PBA)	A method used in risk analysis, that combines probability theory and interval arithmetic to propagate both aleatoric and epistemic uncertainty that has been widely in solving environmental risk assessment problems.
Probability-box p-box	Charting at 0-100th percentile that provides lower and upper bounds on the cumulative probability distribution function (CDF) of an uncertain parameter.
Proppant	A component of the hydraulic fracturing fluid system comprised of sand, ceramics or other granular material that "prop" open fractures to prevent them from closing when the injection is stopped.
Reserves	Reserves are a proven resource that can be economically extracted with current technologies.
Reservoir	A geological formation with adequate porosity, fractures or joints that can store hydrocarbons.
Risk	Combination of possible consequences and associated uncertainties of any action/activity.
Risk assessment	Calculating the impact, magnitude and probability of risks. Often completed to determine if the action/activity should be undertaken or if the action/activity needs to be redesigned.
Risk likelihood	Probability of an impact (physical, environmental, financial) associated with a risk.
Shale gas	Natural gas trapped in a clay rich fine grained sedimentary rock, typically found at depths greater than 1,500m. https://gisera.csiro.au/more-information/frequently-asked-questions/what-is-shale-gas-in-australia/
Tight gas	Hydrocarbon (gas) that is trapped in low porosity and low permeable reservoirs. The reservoir usually requires hydraulic fracturing stimulation to enable economic recovery.
Unconventional gas	Petroleum gas resource that cannot be developed using conventional gas technologies. Includes coal seam gas, shale gas and tight gas.

Well	A hole drilled in to the earth from which hydrocarbons or other fluids can be produced.
Well completion	The assembly of downhole casing/cement and/or other tubing to allow safe and efficient production from a well.
Wellbore delamination	Failure of the wellbore steel casing/cement/rock interface.
Youngs Modulus	Describes the stiffness of the rock, the ratio of the axial stress to axial stain under conditions of uniaxial stress.

References

Adachi, J. et al. 2007. Computer simulation of hydraulic fractures. *International Journal of Rock Mechanics and Mining Sciences* 44(5), pp. 739–757. doi: 10.1016/j.ijrmms.2006.11.006.

Adachi, J.I. et al. 2010. Analysis of the classical pseudo-3D model for hydraulic fracture with equilibrium height growth across stress barriers. *International Journal of Rock Mechanics and Mining Sciences* 47(4), pp. 625–639. doi: 10.1016/j.ijrmms.2010.03.008.

AGL, 2013. *Hydrogeological Summary of the Camden Gas Project area*. AGL Energy Ltd. Available at: https://www.agl.com.au/-/media/AGL/About-AGL/Documents/How-We-Source-Energy/Camden-Document-Repository/Water-Studies/20130131-Hydrogeological-Summary-of-the-Camden-Gas-Project-area.pdf

Arrow Energy 2012. *Surat Gas Project EIS, Groundwater Impact Assessment*.

Augustsson, A. and Berger, T. 2014. Assessing the risk of an excess fluoride intake among Swedish children in households with private wells — Expanding static single-source methods to a probabilistic multi-exposure-pathway approach. *Environment International* 68, pp. 192–199. doi: 10.1016/j.envint.2014.03.014.

Australia Pacific LNG Pty Limited. 2014. *Australia Pacific LNG Upstream Phase 1 Stage 2 CSG Water Monitoring and Management Plan.* Brisbane, Australia.

Aven, T. et al. 2007. A decision framework for risk management, with application to the offshore oil and gas industry. *Reliability Engineering & System Safety* 92(4), pp. 433–448. doi: 10.1016/j.ress.2005.12.009.

Behrmann, L.A. and Nolte, K.G. 1998. Perforating Requirements for Fracture Stimulations. In: *SPE Drilling & Completion*., pp. 228–234. doi: 10.2118/59480-PA.

Betrie, G.D. et al. 2015. Ecological risk assessment of acid rock drainage under uncertainty: The fugacity approach. *Environmental Technology & Innovation* 4, pp. 240–247. doi: 10.1016/j.eti.2015.07.004.

Bioregional Assessment Source Dataset 2014. *NSW Trade and Investment CLM - New South Wales well completion reports.* Available at: http://data.bioregionalassessments.gov.au/dataset/85d50f57-37bb-4af5-ab67-4e8849d0cd98.

Birdsell, D.T. et al. 2015. Hydraulic fracturing fluid migration in the subsurface: A review and expanded modeling results. *Water Resources Research* 51(9), pp. 7159–7188. doi: 10.1002/2015WR017810.

A.P. Bunger, J. Kear, B. Lecampion, and D. Quesada. 2010 The geometry of a hydraulic fracture growing along a wellbore annulus, *9th HSTAM International Congress on Mechanics, Limassol, Cyprus*

Bonett, A. and Pafitis, D. 1996. *Getting to the root of gas migration*.

Chen, Z.R. and Jeffrey, R.G. 2009. Tilt Monitoring of Hydraulic Fracture Preconditioning Treatments. *43rd U.S. Rock Mechanics Symposium & 4th U.S. - Canada Rock Mechanics Symposium* . Available at: https://www.onepetro.org/conference-paper/ARMA-09-100 [Accessed: 29 August 2014].

Cook, P. et al. 2013. *Engineering energy: unconventional gas production: a study of shale gas in Australia*. Australian Council of Learned Academies (ACOLA). Available at: https://espace.library.uq.edu.au/view/UQ:320555 [Accessed: 6 November 2017].

Davies, R.J. et al. 2014. Oil and gas wells and their integrity: Implications for shale and unconventional resource exploitation. *Marine and Petroleum Geology* 56, pp. 239–254. doi: 10.1016/j.marpetgeo.2014.03.001.

Department of Environment and Energy 2013. *Surat Gas Expansion Project Decision Overview*. Available at: http://www.environment.gov.au/system/files/news/239c9cb7-0fa5-444c-a9dc-ac64964ec720/files/surat-gas-expansion-project.pdf.

Department of Environment, 2014. *Hydraulic fracturing ('fraccing') techniques, including reporting requirements and governance arrangements, Background review, Commonwealth of Australia 2014*. Available at: http://www.environment.gov.au/water/publications/background-review-hydraulic-fracturing

Department of Environment and Heritage Protection 2014. Environmental impact statement Ironbark Project. Available at: https://www.ehp.qld.gov.au/management/impact-assessment/eis-processes/ironbark_project.html.

Department of Industry NSW 1998. *Coal Seam Gas Boreholes*. NSW Government. Available at: https://datasets.seed.nsw.gov.au/dataset/c6d29a18-951b-4bb5-8d98-02e9a6625ef0.

Department of Industry NSW 2016. *Coal Seam Gas Boreholes Seed Map*. Available at: https://datasets.seed.nsw.gov.au/dataset/c6d29a18-951b-4bb5-8d98-02e9a6625ef0.

Department of Natural Resources and Mines 2014. Safety advisory—Drilling water bores in coal seam gas areas. Available at: https://www.dnrm.qld.gov.au/__data/assets/pdf_file/0020/224408/safety-drilling-water-bores-csg-areas.pdf (Accessed 18 October 2017).

Department of Natural Resources and Mines 2016. *Underground Water Impact Report for the Surat Cumulative Management Area.* State of Queensland.

Department of Natural Resources Mines. 2017b. *Coal seam gas well locations - Queensland*. State of Queensland. Available at: http://qldspatial.information.qld.gov.au/catalogue/.

Department of Natural Resources and Mines 2017c. *Queensland's petroleum and coal seam gas*. Queensland Government.

Department of Natural Resources and Mines 2017d. *Code of Practice for Constructing and Abandoning Coal Seam Gas Wells in Queensland.* State of Queensland. Available at: https://www.business.qld.gov.au/industries/mining-energy-water/resources/safety-health/petroleum-gas/operating-plant/well-safety.

Department of Natural Resources, Mines and Energy 2017a (DNRME). *Coal seam gas production API*. State of Queensland.

Department of Natural Resources Mines and Energy 2017b (DNRME). *Groundwater Database – Queensland*. State of Queensland. Available at https://data.qld.gov.au/dataset/groundwater-database-queensland

Department of Natural Resources, Mines and Energy (DNRME) 2018. *Direct correspondence.*

Department of Trade and Investment, NSW 2012. *Code of Practice for Coal Seam Gas Well Integrity.* State of New South Wales. Available at: http://www.resourcesandenergy.nsw.gov.au/__data/assets/pdf_file/0006/516174/Code-of-Practice-for-Coal-Seam-Gas-Well-Integrity.PDF.

Draper, J.J. and Boreham, C.J. 2006. GEOLOGICAL CONTROLS ON EXPLOITABLE COAL SEAM GAS DISTRIBUTION IN QUEENSLAND. *The APPEA Journal* 46(1), pp. 343–366.

Dusseault, M.B. et al. 2000. Why Oilwells Leak : Cement Behavior and Long-Term Consequences. *SPE International Oil and Gas Conference and Exhibition, SPE 64733* (SPE-64733), p. 8. doi: 10.2118/64733-MS.

Economides, M.J. and Nolte, K.G. eds. 2000. *Reservoir Stimulation , 3rd Edition*. 3 edition. Chichester, England ; New York: Wiley.

Ferson, S. 2000. *RAMAS risk calc 4.0 software: risk assessment with uncertain numbers*.

Ferson, S. and Ginzburg, L.R. 1996. Different methods are needed to propagate ignorance and variability. *Reliability Engineering & System Safety* 54(2), pp. 133–144. doi: 10.1016/S0951-8320(96)00071-3.

Ferson, S. and Hajagos, J.G. 2004. Arithmetic with uncertain numbers: rigorous and (often) best possible answers. *Reliability Engineering & System Safety* 85(1), pp. 135–152. doi: 10.1016/j.ress.2004.03.008.

Flottman, T. et al. 2013. Influence of in Situ Stresses on Fracture Stimulation in the Surat Basin, Southeast Queensland. In: *SPE-167064-MS*. SPE: Society of Petroleum Engineers. doi: 10.2118/167064-MS.

Fourmaintraux, D.M. et al. 2005. Efficient Wellbore Cement Sheath Design Using the SRC (System Response Curve) Method. In: *SPE-94176-MS*. SPE: Society of Petroleum Engineers. doi: 10.2118/94176-MS.

Frank, M.J. et al. 1987. Best-possible bounds for the distribution of a sum — a problem of Kolmogorov. *Probability Theory and Related Fields* 74(2), pp. 199–211. doi: 10.1007/BF00569989.

Fung, R.L. et al. 1987. Calculation of Vertical Fracture Containment in Layered Formations. *SPE Formation Evaluation* (December), pp. 518–522.

GasFields Commission 2014. *Onshore Gas Well Integrity in Queensland, Australia*. Queensland.

GasFields Commission 2018. *Queensland's Petroleum & Gas Industry Snapshot*. Available at: http://www.gasfieldscommissionqld.org.au/resources/documents/Industry%20snapshot%20FINAL_web%20version.pdf

Geoscience Australia and Australian Stratigraphy Commission 2017. *Australian Stratigraphic Units Database*. Australia. Available at: http://www.ga.gov.au/products-services/data-applications/reference-databases/stratigraphic-units.html.

Geoscience Australia 2016. *Australian Energy Resources Assessment*. Available at: http://aera.ga.gov.au/ [Accessed 5 Feb 2018]

Geoscience Australia 2017. Offshore Eastern Australia Basins - Geoscience Australia. Available at http://www.ga.gov.au/scientific-topics/energy/province-sedimentary-basin-geology/petroleum/offshore-eastern-australia [Accessed 20 October 2017]

Geoscience Australia and BREE (2012) Australia Gas Resource Assessment 2012. Geoscience Australia and the Bureau of Resource and Energy Economics, Canberra.

Geoscience Information of Geological Survey of Queensland 2016. *Well completion reports*. Department of Natural Resources and Mines. State of Queensland. Available at: https://www.business.qld.gov.au/industries/mining-energy-water/resources/online-services/qdex-reports.

GISERA, 2018. *How is onshore gas extracted*? Accessed online March 2018. Available at https://gisera.csiro.au/more-information/frequently-asked-questions/how-is-onshore-gas-extracted/

Goodwin, K.J. and Crook, R.J. 1992. Cement Sheath Stress Failure. *SPE-20453-PA* . doi: 10.2118/20453-PA.

Guner, D. et al. 2017. Investigation of the elastic material properties of Class G cement. *Structural Concrete* 18(1), pp. 84–91. doi: 10.1002/suco.201600020.

Huddlestone-Holmes, CR, Wu, B, Kear, J, and Pandurangan, R. 2017. Report into the shale gas well life cycle and well integrity. EP179028. CSIRO, Australia.

Ingraffea, A.R. et al. 2014. Assessment and risk analysis of casing and cement impairment in oil and gas wells in Pennsylvania, 2000–2012. *Proceedings of the National Academy of Sciences* 111(30), pp. 10955–10960. doi: 10.1073/pnas.1323422111.

ISO 31000:2009 2009. *Risk management — Principles and guidelines*. International Organization for Standardization, Geneva, Switzerland.

Jackson, R.B. et al. 2013. Increased stray gas abundance in a subset of drinking water wells near Marcellus shale gas extraction. *Proceedings of the National Academy of Sciences* 110(28), pp. 11250–11255. doi: 10.1073/pnas.1221635110.

Jeffrey, R.G. et al. 2013. Monitoring and Measuring Hydraulic Fracturing Growth During Preconditioning of a Roof Rock over a Coal Longwall Panel. Available at: http://www.intechopen.com/books/effective-and-sustainable-hydraulic-fracturing/monitoring-and-measuring-hydraulic-fracturing-growth-during-preconditioning-of-a-roof-rock-over-a-co [Accessed: 15 March 2017].

Karanki, D.R. et al. 2009. Uncertainty analysis based on probability bounds (p-box) approach in probabilistic safety assessment. *Risk Analysis: An Official Publication of the Society for Risk Analysis* 29(5), pp. 662–675. doi: 10.1111/j.1539-6924.2009.01221.x.

Kirk-Burnnand, E. et al. 2015. Hydraulic Fracture Design Optimization in Low Permeability Coals, Surat Basin, Australia. In: *SPE-176895-MS*. SPE: Society of Petroleum Engineers. doi: 10.2118/176895-MS.

Lecampion, B. et al. 2013. Interface debonding driven by fluid injection in a cased and cemented wellbore: Modeling and experiments. *International Journal of Greenhouse Gas Control* 18, pp. 208–223. doi: 10.1016/j.ijggc.2013.07.012.

Li, Q. et al. 2015. A review on hydraulic fracturing of unconventional reservoir. *Petroleum* 1(1), pp. 8–15. doi: 10.1016/j.petlm.2015.03.008.

Loizzo, M. et al. 2011. Quantifying the Risk of CO2 Leakage Through Wellbores. *SPE-139635-PA* . doi: 10.2118/139635-PA.

Maloney, D.A. 2015. Unconventional oil and gas in Australia: a case of regulatory lag. *Journal of Energy & Natural Resources Law* 33(4), pp. 349–404. doi: 10.1080/02646811.2015.1089112.

Miyazaki, B. 2009. Well integrity: An overlooked source of risk and liability for underground natural gas storage. Lessons learned from incidents in the USA. *Geological Society, London, Special Publications* 313(1), pp. 163–172. doi: 10.1144/SP313.11.

Montgomery, C.T. and Smith, M.B. 2010. Hydraulic Fracturing: History Of An Enduring Technology. *Journal of Petroleum Technology* 62(12), pp. 26–40. doi: 10.2118/1210-0026-JPT.

Moore, L.P. et al. 2012. Evaluation of Precompletion Annular Gas Leaks in a Marcellus Lateral. In: *SPE-153142-MS*. SPE: Society of Petroleum Engineers. doi: 10.2118/153142-MS.

Nordgren, R.P. 1972. Propagation of a Vertical Hydraulic Fracture. *SPE-3009-PA* . doi: 10.2118/3009-PA.

NSW ground water data archive 2010. *Pinneena, Version 3.2 – Groundwater works*. NSW Office of Water, Department of Environment, Climate Change and Water. Available at: http://waterinfo.nsw.gov.au/pinneena/gw.shtml.

NSW Office of Water. 2013. Water and Coal Seam Gas: Fact Sheet 2, How coal seam gas is extracted. Available at: https://www.water.nsw.gov.au/__data/assets/pdf_file/0011/548048/groundwater_coal_seam_gas_extraction.pdf. [Accessed 3 November 2017]

NSW Parliament 2011. Supplementary Questions AGL Energy Ltd. Available at: https://www.parliament.nsw.gov.au/committees/DBAssets/InquiryOther/Transcript/6898/AQON%20-%20AGL%20Energy%20Limited%20-%2021%20Dec%202011.PDF.

NSW Parliamentary Research Service 2013. *Gas: resources, industry structure and domestic reservation policies. Briefing Paper*.

NT Parliament 2017. *Scientific Inquiry into Hydraulic Fracturing in the Northern Territory. Background and Issues Paper.* Hydraulic Fracking Inquiry, Darwin.

Office of Groundwater Impact Assessment 2016. *Groundwater connectivity between the Condamine Alluvium and the Walloon Coal Measures. A hydrogeological investigation report.* Department of Natural Resources and Mines. State of Queensland.

Office of the Chief Economist 2015. *Review of the socioeconomic impacts of coal seam gas in Queensland.* Commonwealth Department of Industry, Innovation and Science.

Office of the Chief Economist 2016. *Australian Energy Statistics. Australian Government*. Department of Industry, Innovation and Science.

O'Kane, M. 2014. *Final Report of the Independent Review of Coal Seam Gas Activities in NSW.* NSW Chief Scientist and Engineer, Sydney.

Pandey, V.J. et al. 2017. Applications of Geomechanics to Hydraulic Fracturing: Case Studies From Coal Stimulations. *SPE Production & Operations* . Available at: https://www.onepetro.org/journal-paper/SPE-173378-PA [Accessed: 23 October 2017].

Pandey, V. J., & Agreda, A. J. (2014). New Fracture-Stimulation Designs and Completion Techniques Result in Better Performance of Shallow Chittim Ranch Wells. SPE Production & Operations, 29(04), 288-309.

Papendick, S.L. et al. 2011. Biogenic methane potential for Surat Basin, Queensland coal seams. *International Journal of Coal Geology* 88(2), pp. 123–134. doi: 10.1016/j.coal.2011.09.005.

Parcevaux, P. et al. 1990. 8 Prevention of Annular Gas Migration. In: Nelson, E. B. ed. *Developments in Petroleum Science*. Well Cementing. Elsevier, pp. 8–1. Available at: http://www.sciencedirect.com/science/article/pii/S0376736109703061.

Parliament of Victoria 2017. Resources Legislation Amendment (Fracking Ban) Act 2017.

Patel, S. et al. 2015. *Review of Well Integrity in Western Australia*. Petroleum in Western Australia., p. 24–31.

Peirce, A. 2015. Modeling multi-scale processes in hydraulic fracture propagation using the implicit level set algorithm. *Computer Methods in Applied Mechanics and Engineering* 283, pp. 881–908. doi: 10.1016/j.cma.2014.08.024.

Perkins, T.K. and Kern, L.R. 1961. Widths of Hydraulic Fractures. *SPE-89-PA* . doi: 10.2118/89-PA.

Pinetown, K. et al. 2014. *Coal and coal seam gas resource assessment for the Gwydir subregion. Product 1.2 for the Gwydir subregion from the Northern Inland Catchments Bioregional Assessment.* Australia: Department of the Environment, Bureau of Meteorology, CSIRO and Geoscience Australia.

Pollard, D.D. and Fletcher, R.C. 2005. *Fundamentals of Structural Geology*. Cambridge University Press.

QGC Limited 2009. *Queensland Curtis LNG – environmental impact statement*. Brisbane, Australia.

Queensland Competition Authority 2014. *Coal Seam Gas Review Final Report.* Government of Queensland, Brisbane.

Raiber, M. et al. 2016. *Conceptual modelling for the Clarence-Moreton bioregion. Product 2.3 from the Clarence-Moreton Bioregional Assessment.* Australia: Department of the Environment and Energy, Bureau of Meteorology, CSIRO and Geoscience Australia. Available at: http://data.bioregionalassessments.gov.au/product/CLM/CLM/2.3.

Ransley, T. et al. 2015. Groundwater Hydrochemical Characterisation of the Surat Region and Laura Basin - Queensland : Final technical report for the National Collaboration Framework Hydrochemical Characterisation Project. Available at: https://data.gov.au/dataset/groundwater-hydrochemical-characterisation-of-the-surat-region-and-laura-basin-queensland-final [Accessed: 6 November 2017].

Rozell, D.J. and Reaven, S.J., 2012. Water pollution risk associated with natural gas extraction from the Marcellus Shale. Risk Analysis, 32(8), pp.1382-1393.

SA Parliament, Natural Resources Committee 2016. *Inquiry into Unconventional Gas (Fracking) in the South East of South Australia Final Report*. Parliament of South Australia, Adelaide.

Sander, P. et al. 2006. Uncertain numbers and uncertainty in the selection of input distributions--consequences for a probabilistic risk assessment of contaminated land. *Risk Analysis: An Official Publication of the Society for Risk Analysis* 26(5), pp. 1363–1375. doi: 10.1111/j.1539-6924.2006.00808.x.

Sander, R. et al. 2014. *Coal and coal seam gas resource assessment for the Maranoa-Balonne-Condamine subregion. Product 1.2 for the Maranoa-Balonne-Condamine subregion from the Northern Inland Catchments Bioregional Assessment.* Australia: Department of the Environment, Bureau of Meteorology, CSIRO and Geoscience Australia.

Scott, S. et al. 2007. Coal petrology and coal seam gas contents of the Walloon Subgroup — Surat Basin, Queensland, Australia. *International Journal of Coal Geology* 70(1), pp. 209–222. doi: 10.1016/j.coal.2006.04.010.

Scott, S. G. (2008). The geology, stratigraphy and coal seam gas characteristics of the Walloon subgroup-Northeastern Surat Basin (Doctoral dissertation, James Cook University).

Taoutaou, S. 2010. Well Integrity - Expert View | ArabianOilandGas.com, http://www.arabianoilandgas.com/article-6920-well-integrity--expert-view/. Available at: http://www.arabianoilandgas.com/article-6920-well-integrity-expert-view/ [Accessed: 5 October 2017].

Tas. Department of Primary Industries, Parks, Water and Environment 2015. *Review of Hydraulic Fracturing in Tasmania Final Report.* Government of Tasmania, Hobart.

Thorogood, J.L. and Younger, P.L. 2015. Discussion of 'Oil and gas wells and their integrity: Implications for shale and unconventional resource exploitation' by R.J. Davies, S. Almond, R.S., Ward, R.B. Jackson, C. Adams, F. Worrall, L.G. Herringshaw, J.G. Gluyas and M.A. Whitehead. *Marine and Petroleum Geology* 59(February), pp. 671–673. doi: 10.1016/j.marpetgeo.2014.07.011.

U.S. EPA 2016. *Hydraulic Fracturing for Oil and Gas: Impacts from the Hydraulic Fracturing Water Cycle on Drinking Water Resources in the United States (Final Report).* U.S. Environmental Protection Agency, Washington, DC,.

US EPA. 2015. Report: Retrospective Case Study in Killdeer, North Dakota (PDF). Available at: https://www.epa.gov/hfstudy/report-retrospective-case-study-killdeer-north-dakota-pdf [Accessed: 5 October 2017].

Valkó, P. and Michael J., E. 1995. *Hydraulic fracture mechanics.* New York: Wiley.

Vic. Environment and Planning Committee, (first) 2015. *Inquiry into Onshore Unconventional Gas in Victoria Final Report*. Parliament of Victoria, Melbourne.

WA Standing Committee on Environment and Public Affairs 2015. *Implications for Western Australia of Hydraulic Fracturing for Unconventional Gas. Report 42,*. Parliament of Western Australia, Perth.

Watson, T. et al. 2002. Specialized Cement Design and Placement Procedures Prove Successful for Mitigating Casing Vent Flows - Case Histories. In: *SPE-76333-MS*. SPE: Society of Petroleum Engineers. doi: 10.2118/76333-MS.

Watson, T.L. and Bachu, S. 2009. Evaluation of the Potential for Gas and CO2 Leakage Along Wellbores. *SPE-106817-PA* . doi: 10.2118/106817-PA.

Welsh, W. et al. 2014. Context statement for the Maranoa-Balonne-Condamine subregion, Product 1.1 for the Maranoa-Balonne-Condamine subregion from the Northern Inland Catchments. Bioregional Assessment.

Williamson, R.C. and Downs, T. 1990. Probabilistic arithmetic. I. Numerical methods for calculating convolutions and dependency bounds. *International Journal of Approximate Reasoning* 4(2), pp. 89–158. doi: 10.1016/0888-613X(90)90022-T.

Yager, R.R. 1986. Arithmetic and other operations on Dempster-Shafer structures. *International Journal of Man-Machine Studies* 25(4), pp. 357–366. doi: 10.1016/S0020-7373(86)80066-9.

Zhang, M. and Bachu, S. 2011. Review of integrity of existing wells in relation to CO2 geological storage: What do we know? *International Journal of Greenhouse Gas Control* 5(4), pp. 826–840. doi: 10.1016/j.ijggc.2010.11.006.

Appendix A: Hydraulic fracture numerical models

The oil and gas industry uses a number of analytical and numerical hydraulic fracture models to simulate the propagation of hydraulic fractures in the field (Economides and Nolte 2000; Adachi et al. 2007). The equilibrium height growth model is based on a 2D plane strain analysis of the fracture height in a layered-stresses system where material property variations are neglected (Fung et al. 1987). The "pseudo-3D" (P3D) model, which is widely used in the petroleum industry, was introduced to simulate the propagation of a vertical hydraulic using the equilibrium height growth model (Adachi et al. 2010).

Hydraulic fracturing involves a number of mechanical processes such as rock deformation, fluid flow and fracture propagation which are computationally intensive to model. Modelling challenges are further compounded by a number of factors such as the presences of multiple rock layers with different material properties, non-homogeneous stress conditions, formation permeability, stress shadows from previous fractures, soft coal seams, and fluid loss to natural fractures. Numerical models typically simplify the problem by not considering some of these mechanics. The PKN and the penny shaped models are simple fracture models that are built on assumptions which have specific limitations. For instance, the PKN model has the following assumptions;

- the stresses in the layers above and below the pay zone are sufficiently large to prevent hydraulic fracture growth out of the pay zone,
- mechanical effects of the hydraulic fracture tip are not considered,
- the rock is assumed to be a homogeneous and elastic mass, and
- parameters such as rock porosity, surface roughness, tortuosity, fluid friction loss at the entrance and the effect of filter cake are not considered.

These assumptions may explain why the hydraulic fracture geometry predicted by simulators/numerical models may not agree with field observations. For example, in the recent fracturing trials carried out in Surat basin, the fracture height predicted by fracture simulators were off by more than 100% compared to micro-seismic results (Pandey et al. 2017).

PKN

The PKN model is a pseudo-3D model that assumes a constant height h_f and predicts the fracture opening and the length as a function of time. The model also assumes an independent deformation cross-section based on the hypothesis that plane strain conditions are valid along every vertical plane normal to the direction of fracture propagation, and neglects the variation of pressure along the verticWal co-ordinate. For such a planar fracture propagating in an infinite homogeneous, linear elastic isotropic medium, the net pressure $\mathrm{p_n}$ which is the pressure in excess of the far-field confining stress, along the lateral x direction at any time t can be related to the maximum fracture opening w of each cross-section as

$$\mathrm{w(x,t)} = \frac{2p_n h_f}{E'} \tag{1}$$

where E' is the plane strain modulus.

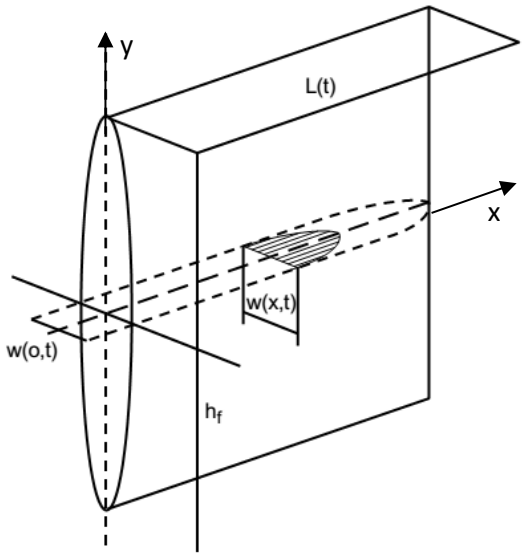

Figure 23 - Schematic of a PKN Fracture (Adapted from Economides and Nolte (2000))

Because the fluid flow is one dimensional along the fracture length in the PKN model, the pressure drop within the fracture for a Newtonian fluid can be obtained from the Hagen–Poiseuille equation as

$$\frac{\partial \mathrm{P_n}}{\partial \mathrm{x}} = -\frac{64\mu \mathrm{q}}{\pi \mathrm{h_f w^3}} \tag{2}$$

where μ is the fluid viscosity and q the flow rate across the horizontal cross-section.

Equations (1) and (2) coupled with the mass balance requirement can be solved to obtain the fracture opening w by using the assumption that the flow rate at the inlet is half the injection rate Q (only one wing of the fracture is considered due to geometrical symmetry). Mass balance implies that the volume of the injected fluid should equal the sum of the volume of the generated fracture and the volume of fluid lost to the surrounding rock. In the case of the PKN model with a constant injection rate and no leak-off, the global mass balance can be written as $Qt = 2\bar{w}Lh_f$, where $\bar{w}$ is the fracture opening averaged over the fracture half-length L along the horizontal cross-section.

The energy required for propagating the fracture is primarily supplied by the energy of the injected fluid which gets dissipated during the fracture propagation process both by viscous dissipation as the fluid flows through the fracture, and also during the breakage of the rock. Each of these dissipative processes is associated with a characteristic length scale which leads to a multi-scale solution that is dependent on the propagation regime (Peirce 2015). In the case of hydraulic fracturing treatments carried out under field conditions, it has been found that fracture propagation is dominated by viscous dissipation (Adachi et al. 2007). Therefore, for the current study, we consider the fracture propagation to be in the viscosity dominated regime (zero toughness solution)

without leak-off, for which the steady state solution for the fracture length *L* at large times can be obtained (Nordgren 1972).

$$L(\mathrm{t}) = 0.59 \left(\frac{E' Q^3}{\mu \mathrm{h}^4}\right)^{\frac{1}{5}} t^{\frac{4}{5}} \tag{3}$$

Penny-shaped

The penny shaped model is more appropriate when the height growth is not constrained or when the fractures are horizontal. The governing equations are same as before and the evolution of the fracture radius R can be obtained in a similar fashion (Economides and Nolte 2000).

$$R(t) = 0.52 \left(\frac{E' Q^3}{\mu}\right)^{1/9} t^{\frac{4}{9}} \tag{4}$$

Appendix B: Wellbore delamination model

The governing equations for the problem consists of the elasticity equation that relates the net pressure in the annulus and its opening. For an interface crack having constant arc length 2ϑ with axial length l much larger than the arc length, assuming plane strain condition at every horizontal cross-section and uniform net pressure p, the crack opening displacement w can be written as,

$$w(\theta) = 2\vartheta RF(\theta, \vartheta)\frac{p}{M}, \theta \in [-\vartheta, +\vartheta] \tag{5}$$

where the net pressure p is the pressure inside the micro-annuls in excess of the clamping stress σ_n along the interface, F is a dimensionless function of the crack arc-length and M is the equivalent elastic modulus, both of which are functions of the mechanical properties of casing and the cement material, and also the geometry of the wellbore. For the completely debonded case ($\vartheta = \pi$), the equivalent elastic modulus can be obtained from the classical Lamé solution for cylinders subject to constant pressure under plane strain conditions.

$$\frac{1}{M} = \frac{2R_1^2+R_2^2(\lambda 1-1)}{4\mu_1(R_2^2-R_1^2)} + \frac{R_2^2(\mu 2-\mu 3)(\lambda_2-1)+R_3^2(2\mu_2+\mu_3(\lambda_2-1))}{2\mu_2\left(2R_2^2(\mu_3-\mu_2)+R_3^2(2\mu 2+\mu 3(\lambda_2-1))\right)} \tag{6}$$

where $\mu = E/2(1+\nu)$ is the elastic shear modulus, ν the Poisson's ratio, λ and μ Lame constants, and subscripts 1, 2 & 3 correspond to the casing, cement and rock respectively.

Next, the fluid flow within the annuli is assumed to be unidirectional and laminar and modelled using the Reynold lubrication theory. The fluid flux per unit arc length is obtained by combining the continuity equation for the mass conservation over any cross section, and the Poiseuille law that relates the fluid-flux to the pressure drop and opening in the annulus.

$$q = -\frac{w_o^3}{\mu'}\left(\frac{\partial p}{\partial z} - B\right) \tag{7}$$

where μ' is the equivalent fluid viscosity and B is a stress gradient term that expresses the buoyancy contrast between the casing and the micro annuli.

The elasticity and fluid flow equations (6) and (7) coupled with the mass balance equation, are solved to obtain the evolution of the crack opening, fluid flux with the crack, and the crack length, by assuming that the injection pressure p_{inj} is constant at the inlet of the crack or at the bottom of the wellbore, both the flux and the crack opening vanish at the tip, and there is no fluid lag.

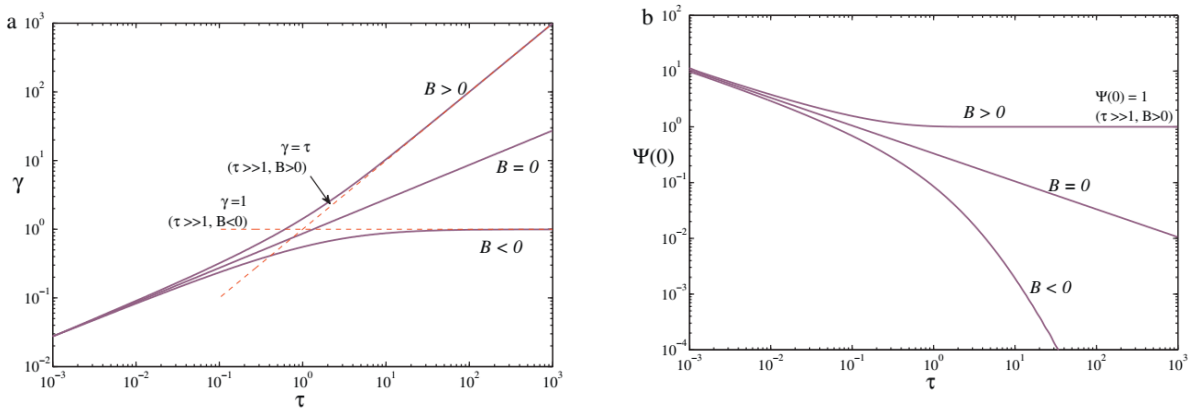

Figure 24 - Evolution of dimensionless fracture length (left) and the dimensionless flux entering the fracture (right). (Adapted from Lecampion et al. (2013))

Figure 24 shows the results for the evolution of the dimensionless fracture length γ and the dimensionless flux Ψ entering the micro-annulus as a function of the dimensionless time τ. The solutions highlight three regimes of propagation: a "pressure driven" regime at early times where the fracture length is small and the fluid flux is driven by the pressure gradient. At larger times ($\tau \gg 1$), the pressure driven regime gives way to either a "buoyancy limited" regime where the stress gradient term B<0, or "buoyancy driven" regime where B>0. In the buoyancy limited regime, the fluid flux tends to zero, where as in the buoyancy driven regime the fluid continues to be driven up the annulus. Similarly, in the buoyancy limited regime, fracture growth stops in a finite time when buoyant force reach equilibrium against the pressure, whereas for the buoyancy driven case, the crack velocity increases with time, and the dimensionless fracture length evolves as $\tau^{1/2}$ at small times and evolves as τ at larger times.

The objective is to determine the evolution of a micro-annuli of radius *R* at a depth *Z* from the ground surface which is subject to a constant fluid pressure p.

Dimensionless scaling is mainly introduced to obtain a numerical solution. The dimensionless solution can be easily be converted into real units using the corresponding characteristic scaling. In the current study, the objective is to assess the risks due to wellbore delamination by investigating the possibility of a micro-annuli crack propagating between the cement/casing or cement/rock interfaces driven either by the hydraulic fracturing pressure during the stimulation or the constant reservoir pore pressure after decommissioning.

Appendix C: Probability box

The probability box (*p-box)* approach provides lower and upper bounds on the cumulative probability distribution function (CDF) of an uncertain parameter. Uncertainty propagation is carried out by combining *aleatoric* and *epistemic* uncertainty to generate a probability distribution for the different interval limits. For example, the top left graph in Figure 25 shows a variable Y_1 whose value is known to lie within a range between 3 and 8. The lower and upper CDF bounds are shown in red and green respectively. The top right graph in Figure 25 shows Y_2 which is well described by a lognormal probability distribution with a mean and variance of 1.61 and 0.42 respectively. The CDF of the variable Y_2 has been truncated at the 5th and 99th percentiles. The bottom two graphs in Figure 26 show the *p-boxes* generated for the product $Z_1 = Y_1.Y_2$ and the sum $Z_2 = Y_1 + Y_2$. It can be observed that the answer is not a single CDF, rather a region within which the CDF of the product or the sum lies. Irrespective of the true value of the variable Y1 or Y2, the CDF of the product and sum lies somewhere within the region identified by the upper and lower CDFs, also known as probability box or *p-box*. The result expresses both *epistemic* uncertainty (Y_1) and *aleatoric* uncertainty (Y_2) in a single graph. The horizontal span between the bounds representing the epistemic uncertainty, and the vertical slant representing variability in the aleatory uncertainty.

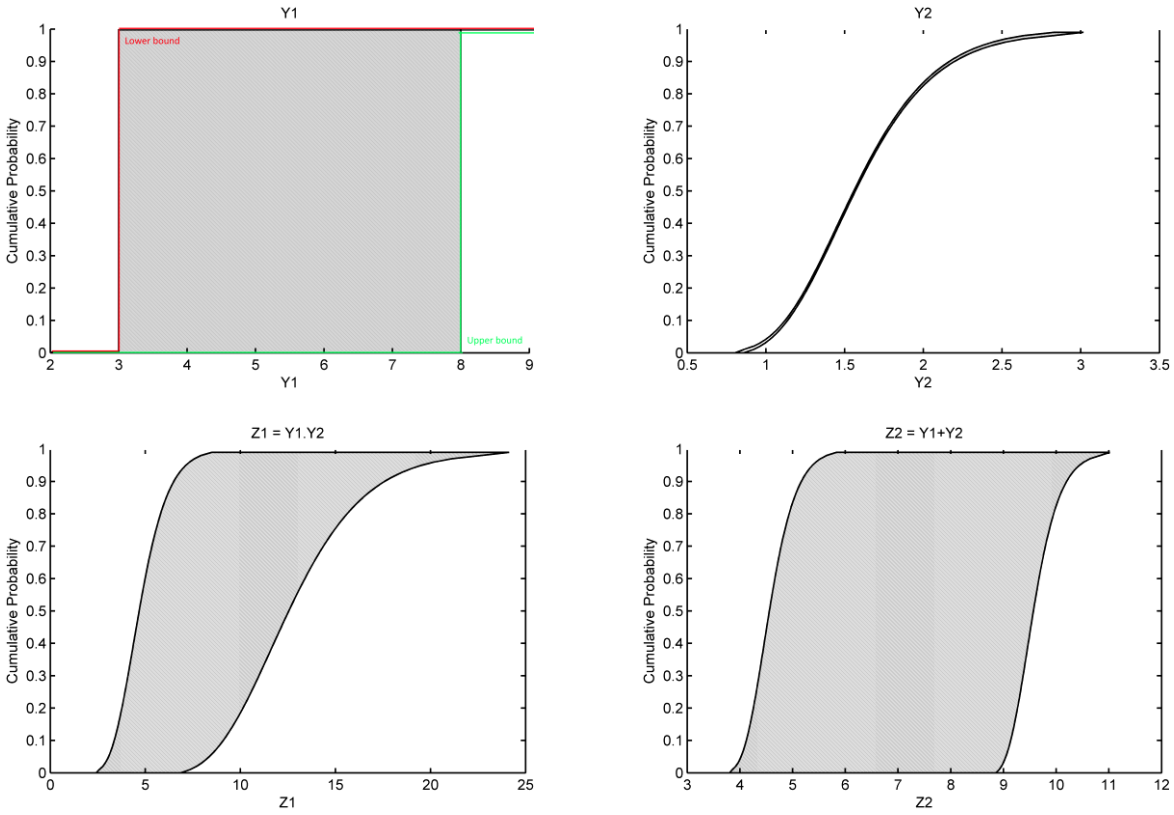

Figure 25 - Top: Distribution for the variable Y_1: an interval representing epistemic uncertainty (no knowledge of distribution); and Y_2 which is lognormal CDF with mean 1.61 and variance 0.42 representing aleatory uncertainty (known distribution). Bottom: Probability box (*p*-box) for the product $Z_1 = Y_1.Y_2$ and the sum $Z_2 = Y_1 + Y_2$.

Under a Monte Carlo simulation where values are generated, the CDF of variables Y1 and Y2 would be enclosed by the *p-box*. Alternatively, for a two phase Monte Carlo simulation that considers both *epistemic* and *aleatoric* uncertainties, the result would also be enclosed by the *p-box* (Karanki et al. 2009). However, the *p-box* approach is computationally more efficient than a typical Monte Carlo simulation and better suited when little information is available about the parameter distribution and/or their dependencies (Karanki et al. 2009).

CONTACT US

t 1300 363 400
+61 3 9545 2176
e csiroenquiries@csiro.au
w www.csiro.au

AT CSIRO, WE DO THE EXTRAORDINARY EVERY DAY

We innovate for tomorrow and help improve today – for our customers, all Australians and the world.

Our innovations contribute billions of dollars to the Australian economy every year. As the largest patent holder in the nation, our vast wealth of intellectual property has led to more than 150 spin-off companies.

With more than 5,000 experts and a burning desire to get things done, we are Australia's catalyst for innovation.

CSIRO. WE IMAGINE. WE COLLABORATE. WE INNOVATE.

FOR FURTHER INFORMATION

Energy
Dane Kasperczyk
t +61 3 9545 2411
e dane.kasperczyk@csiro.au
w research.csiro.au/oilandgas